ADDITION OF A STANTON GAUGE TO THE BOUNDARY LAYER DATA SYSTEM

A Thesis

presented to

the Faculty of California Polytechnic State University,

San Luis Obispo

In Partial Fulfillment

of the Requirements for the Degree

Master of Science in Mechanical Engineering

by

Brittany Reanne Kinkade

June 2014

COMMITTEE MEMBERSHIP

TITLE:	Addition of a Stanton Gauge to the Boundary Layer Data System
AUTHOR:	Brittany Reanne Kinkade
DATE SUBMITTED:	June 2014
COMMITTEE CHAIR:	Dr. Russell Westphal, Professor Mechanical Engineering Department
COMMITTEE MEMBER:	Dr. Rob McDonald, Associate Professor Aerospace Engineering Department
COMMITTEE MEMBER:	Marshall Lee McFarland, Lecturer Mechanical Engineering Department

ABSTRACT

Addition of a Stanton Gauge to the Boundary Layer Data System

Brittany Reanne Kinkade

The Stanton gauge technique provides an indirect method for measurement of skin friction on a smooth aerodynamic surface in which a pressure tap is available. This thesis presents the design and evaluation of a new type of skin friction measurement gauge based on the Stanton gauge concept but not requiring a surface pressure tap. This new skin friction measurement gauge, called a "Flow Tab", can therefore be used on an aerodynamic model or aircraft surface without alteration of the surface. The Flow Tab is thus particularly well-suited to use with Cal Poly's Boundary Layer Data System (BLDS), a small, self-contained instrument that can be installed onto a model or aircraft surface without permanent alteration of the surface. A series of preliminary experiments conducted in a low-speed wind tunnel on a flat plate model with mild favorable pressure gradient, with both laminar and turbulent boundary layers, led to selection of three variants of the Flow Tab design. These Flow Tabs had edge heights of 0.002, 0.0035, and 0.005 inches, giving dimensionless heights h^+ of 1.4 -16 over the streamwise Reynolds number range of about 0.7 to 2.2 million. Uncertainty analysis and test results demonstrated that better than 10% measurement uncertainty for the Flow Tab results could be achieved with edge heights of 0.0035 and 0.005 inches using the same calibration equations as published for the Stanton gauge. Further investigation of its performance over a wider range of Reynolds numbers, and in more complex conditions including those encountered on swept wings with a variety of pressure gradients, is recommended. Integration of the flow tab with BLDS for flight testing applications presents challenges related to its relatively small pressure signal that may require some special modifications to existing BLDS hardware and software.

Keywords: Stanton, Skin Friction, Flow Tab, BLDS, Laminar, Turbulent

ACKNOWLEDGMENTS

I would like to begin by expressing my deepest gratitude to my advisor, Dr. Russ Westphal. Your unfailing enthusiasm and constant support throughout the duration of this project and my entire time as part of the BLDS team has been truly amazing. There simply are no words to describe my appreciation to you. Thank you so very much Russ.

A very special thank you to Jim Gerhardt for his amazing contribution to this project. Your countless hours spent machining unthinkably small parts have made this project possible. Thank you Jim.

I would also like to thank Ladd Caine for his help with my project, it is truly appreciated. Thank you Ladd.

Many thanks to the members of the BLDS team throughout my years working on the project. You all are amazing and it was a pleasure to work with each and every one of you.

I would also like to thank Northrop Grumman Corporation for their support of the BLDS group and of my thesis in particular. Specifically I would like to thank Anne Sullivan and Chris Harris for their tremendous support of the BLDS work.

Final thank you goes to my family who have always been there for me in each and every way possible. I would like to thank my mom and dad for their support throughout my life, without you none of this would be possible. Thank you, I love you so much.

TABLE OF CONTENTS

LIST OF TABLES

LIST OF FIGURES

NOMENCLATURE

b	=	Breadth of blade, m
BLDS	=	Boundary Layer Data System
C_f	=	Skin friction coefficient, dimensionless
d_h	=	Diameter of static hole, m
δ	=	boundary layer thickness, m
h	=	Effective blade height, m
$h+$	=	Dimensionless height
l	=	Length of blade, m
ΔP	=	Differential pressure reading, Pa
ρ	=	Air density, kg/m^3
Re	=	Reynolds number
τ	=	Shear stress at surface, N/m^2
u_τ	=	Shear velocity, m/s
μ	=	Dynamic viscosity, Ns/m^2
V	=	Air flow velocity, m/s
ν	=	Kinematic viscosity, m^2/s
x^*	=	Dimensionless x quantity in Stanton calibration
y^*	=	Dimensionless y quantity in Stanton calibration

1. INTRODUCTION

The objective of this thesis is to develop and evaluate a new capability for the Boundary Layer Data System (BLDS) [1] to measure the skin friction on an aerodynamic surface during in-flight testing using a modified version of the Stanton gauge approach [2]. The BLDS currently uses a Preston tube to measure skin friction and applies both the calibration equations for laminar and turbulent flow regimes to the data to not only determine the skin friction coefficient but also to determine the flow regime itself. The Stanton gauge method would augment the current method in that a single calibration equation is used which is independent of the flow regime. The use of a conventional Stanton gauge would not be suitable for this project because it requires a surface static pressure port, a small hole in the surface over which the skin friction is to be measured, and such a port is often not available in test conditions to which BLDS is applied. This chapter will review the concept of skin friction and its measurement, the conventional Stanton gauge method for measuring skin friction, the requirements for the device to conform to the flight test environment and integration within the BLDS system, and static pressure measurement methods.

1.1 Skin Friction Measurement Technique Overview

The skin friction coefficient over a surface is the local shear stress normalized by the local dynamic pressure. This value gives an indication of the local shearing stress present at the aerodynamic surface of interest [3]. The ability to measure the skin friction on aerodynamic surfaces is paramount when considering design for aerospace

applications as well as serving as a basis for aerodynamic modeling to be compared against for accuracy. Being able to measure the skin friction on a surface allows for insight into the flow itself as well as being able to verify results from computer generated models such as computational fluid dynamics (CFD).

One major application that the skin friction coefficient is used for by the BLDS device is determining whether the flow type of the aerodynamic surface is laminar or turbulent. The Reynolds number of the flow, which is a dimensionless quantity that is the ratio of the dynamic forces to the friction forces, is a key quantity when determining flow type. The Reynolds number is calculated based on fluid velocity, V, body characteristic length, l, fluid density, ρ, and fluid dynamic viscosity, μ. The equation for Reynolds number is as follows:

$$Re = \frac{Vl\rho}{\mu}$$

A laminar boundary layer occurs within a range of low to moderately high Reynolds numbers. With this type of flow the particles of the fluid move essentially parallel to one another with constant local velocities. A turbulent boundary layer will develop at larger Reynolds numbers than that of the laminar boundary layer. In this type of flow the fluid particles are no longer moving in parallel to one another instead they form eddies and oscillate along the surface of interest. The viscous effects on a turbulent boundary layer therefore are much larger and produce larger skin friction coefficients than that of a laminar boundary layer [3]. This large difference in skin friction coefficient between laminar and turbulent flows will be utilized in order to determine the flow regime over the aerodynamic surface. The skin friction will be calculated and, based on

the magnitude of the resulting skin friction coefficient, the flow will be characterized as laminar or turbulent.

Skin friction measurement techniques are divided into two major categories: direct and indirect methods. Hakkinen [4] compiled a survey report detailing the principal categories of techniques for measuring skin friction. White [5] provided a taxonomy of skin friction measurements in his Master's thesis which is reproduced and provided in Table 1-1 below. The table demonstrates various measurement methods that fall under each of the two main categories of direct or indirect methods for measuring skin friction.

Table 1-1. Skin friction measurement methods [5]

Direct Methods	Indirect Methods

• Floating Element
• Oil Film
• τ Liquid Crystal
	• Velocity/Pressure
	  – Clauser Plot
	  – Wall V (PW, HW, LDV)
	  – Preston/ Stanton/ Fence
	• Heat Transfer
	  – Wall Wire/Film
	  – T Liquid Crystal
	• Electrochemical
	• Mass Transfer
	  – Sublimation
	  – Evaporation

1.2 Stanton Gauge ("Razor Blade") Method for Measuring Skin Friction

1.2.1 Development of the Stanton Gauge Method

The use of Stanton gauges began in the late 1920's as a means of measuring the air velocity near an aerodynamic surface. T.E. Stanton [6] and his colleagues developed a means of positioning a Pitot tube as close as possible to the model surface by simply removing one side of the Pitot tube and laying the half-tube on the surface of the model. This essentially replaced the removed side of the Pitot tube with the surface of the model, and these new Pitot tubes were called "surface tubes." The measurement of the difference between the surface tube pressure and the local static pressure, with the latter measured using a static pressure tap in the surface, provided the necessary data from which near-surface velocity could be determined. This concept gave way to additional work to relate the measured velocity, or pressure difference between surface tube and wall static, and the skin friction on the surface itself.

This approach for measuring the velocity profile on an aerodynamic surface eventually led to introduction of razor blades adhered to the surface of a model over a wall static tap in place of the half-Pitot tube by J.N. Hool [7]. In essence, Hool transformed a traditional static pressure hole into a very fine Pitot tube that existed within the model's surface itself. The pressure reading from the altered wall static tap provided what Hool thought to be the total head of the fluid flowing very close to the surface itself, and served as the disturbed pressure reading. When the blade is removed from the surface, the experiment is run again under identical conditions and the undisturbed pressure is measured. The difference between these two measured pressures is then used

in the calibration equations that calculate the skin friction on that surface for those flow conditions considered. The objective of this thesis is to develop a version of this "razor blade" method in the form of a probe that can be used in the absence of any surface static pressure taps. This would allow for Stanton type measurements to be made on a surface without requiring invasive alterations to the surface such as drilling wall static pressure taps.

1.2.2 Method for Measuring Skin Friction

The Stanton gauge, or "razor blade", method is an indirect method of measuring skin friction that uses the pressure differential between a disturbed and an undisturbed wall static tap on the model of interest [8]. A razor blade is cut to an appropriate size, usually less than one inch square, and the blade's sharpened leading edge is positioned atop a wall static tap, creating an obstruction to the flow. This configuration [8] is documented by Campbell and Hanratty [2] and is reproduced in Figure 1-1 below. The pressure read from the altered wall static tap once the razor blade has been adhered over top of it will be higher as a result of the obstruction and is taken as the disturbed pressure reading. The undisturbed surface static pressure reading is taken from an unaltered wall static tap nearby, or from data recorded separately without the installation of the razor blade but under identical flow conditions.

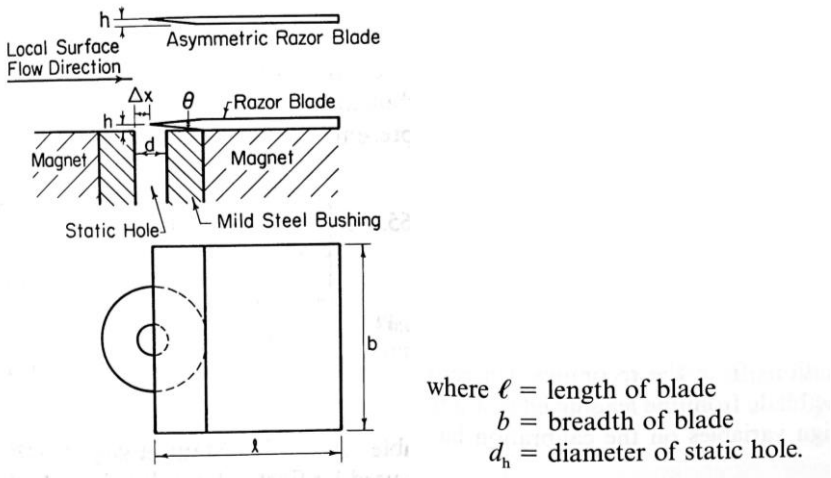

Figure 1-1. Overall design of the Stanton Gauge with pertinent dimensions proposed by East [2] [8]

East [8] provided typical, standard ratios for the relevant dimensions in the razor blade method set up as:

$$\frac{d_h}{h} = 6 \qquad \frac{b}{h} = 36 \qquad \frac{l}{b} = 1 \qquad \frac{\Delta x}{h} = 0$$

Where the variables listed are as demonstrated in the schematic of Figure 1-1. These ratios for the various parameters associated with the razor blade configuration provided acceptable results for skin friction measurements as a result of experimentation conducted by East and his colleagues.

The difference between the disturbed and undisturbed surface static pressures provides the differential pressure for skin friction calculations using published correlations. There are two main calibration correlations that are widely accepted for their accuracy in determining the skin friction coefficient; one for laminar flow regimes and one for turbulent flow regimes. The laminar calibration, developed by J.N. Hool [7]

through experimentation with the Stanton method in laminar flow regimes, utilizes the following dimensionless parameters.

$$x^* \equiv log_{10}\left(\frac{\Delta \bar{P} h^2}{\rho \nu^2}\right)$$

$$y^* \equiv log_{10}\left(\frac{\bar{\tau} h^2}{\rho \nu^2}\right)$$

The calibration equation itself was determined to have the form

$$y^* = -0.130 + 0.625x^*$$

for x* values ranging from -0.85 to 0.2.

The turbulent calibration, developed by East [8] utilizes the same dimensionless quantities and is as follows:

$$y^* = -0.23 + 0.618x^* + 0.0165x^{*2}$$

for x* values ranging from 2 to 6.

A key feature of the correlations is that they are nearly identical, whether carried out in laminar or turbulent flow; it is this feature that has made them so promising for application to measurements during flight research aimed at investigating laminar flow technology. Hool's calibration and East's calibration prove nearly continuous when a plot of the involved dimensionless quantities in the calculations is made that includes both calibration curves together. A plot demonstrating this key element is shown in Figure 1-2 below.

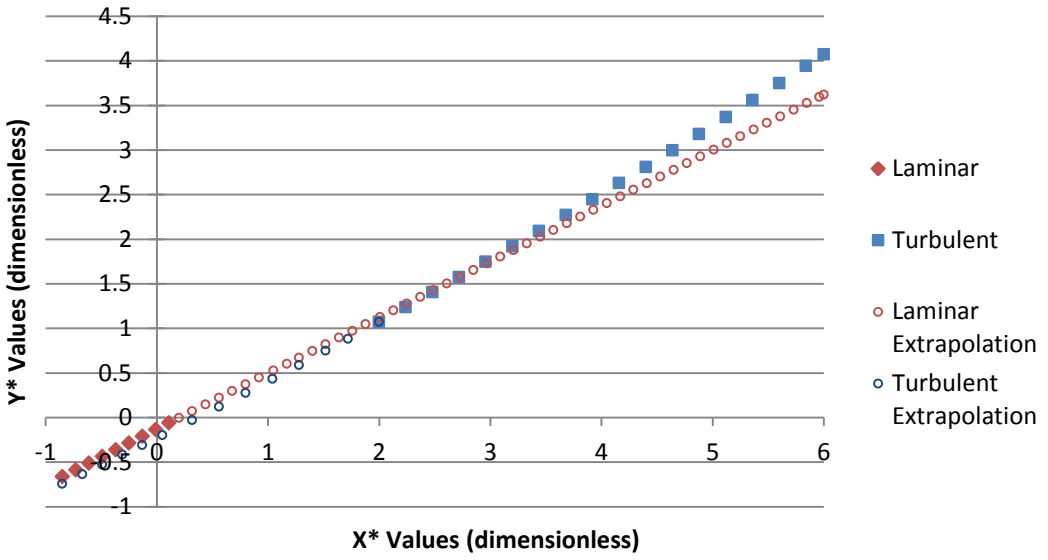

Figure 1-2. Plot demonstrating continuity between laminar and turbulent calibration equations

As seen in the figure above, both the turbulent and laminar correlations provide nearly identical results for the y* values with specific x* value inputs. It is noticeable however that the turbulent correlation, which has a quadratic form, will have noticeably different behavior as the x* value grows large but will match the laminar behavior at low x* values. The laminar correlation, not having the higher order term, will not be able to satisfy this behavior at higher x* values and the two correlations will no longer be nearly identical. The turbulent correlation will be used as the single calibration curve for this project because of its accuracy of calculating y* based on a given x* regardless of the actual flow behavior. Additionally, most of the data collected for this project yielded x* values that were within the range provided for the turbulent correlation therefore use of that correlation was appropriate.

There are two main types of razor blade geometries that can be used with the Stanton method: single-sided, and double-sided. The type of edge on the razor blade

determines the effective height, h, which is used in the calibration relations to compute the skin friction coefficients. With a single-sided blade mounted with its beveled edge facing down the overall thickness of the razor becomes the height, h. With a double-sided blade half of the overall razor thickness is used as the effective height, h. The two configurations are illustrated in Figure 1-3.

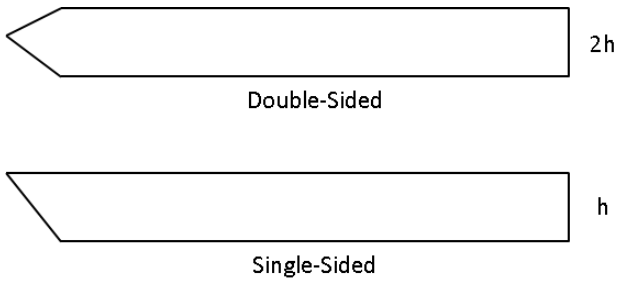

Figure 1-3. Schematic of the two different blade configurations for Stanton gauges

The Stanton method itself rests on the assumption that the effective height of the blade being used is small compared to the boundary layer thickness, δ, of the flow or $h/\delta << 1$ such that it lies within the linear velocity profile portion of the boundary layer [9]. This portion of the boundary layer is an extremely thin region and is referred to as the viscous sublayer [10]. The blade thickness used has typically been less than 0.010 inches; larger values give bigger differential pressures but can exceed the range of validity of the calibration, so the choice of h becomes a trade-off with h values around 0.002-0.005 ins. generally being preferred.

1.3 Project Requirements

1.3.1 Single Calibration Curve for Calculating Skin Friction

It is desired that the skin friction be calculated without respect to the flow regime over the surface of interest. This requires that a single skin friction calibration be used that is independent of whether the flow is laminar or turbulent while still maintaining accurate results for either flow regime. The use of a single calibration equation is convenient in that the flow type on a model of interest is generally not known prior to its measurement and is often a desired result of the experimentation itself. This approach would be advantageous as compared to the Preston tube method, for example. Measurements from a Preston tube are commonly analyzed with both laminar and turbulent calibration equations, then some judgment must be exercised to select which is applicable. For example, if the laminar correlation yields skin friction values that are consistent with laminar flow regime values, it is assumed that the flow was laminar. However, if the laminar correlation yielded a skin friction coefficient that was not consistent with a typical laminar value, it would be assumed that the flow was turbulent, and the results from the turbulent correlation would be evaluated to make sure that they are consistent with typical turbulent skin friction values. The Stanton method for measuring skin friction is an ideal replacement to this method because, as shown above, the laminar and turbulent calibrations published for the Stanton method agree with one another so well that they can be thought of as one continuous function throughout the range of its applicability based on specified non-dimensional quantities.

1.3.2 Skin Friction Probe Requirements

The BLDS device needs to operate in conditions such as wind tunnel and flight testing. During these situations, it is very difficult or sometimes impossible to alter the test surface in order to make certain measurements. Additionally, the idea behind the BLDS device is to be able to collect data on a surface autonomously without interfering with the test surface itself. These requirements present a challenge when considering a Stanton-type device for measuring skin friction because of the nature of the traditional Stanton gauge device. A true wall static tap would need to be installed on the model at the specific locations of interest where the skin friction is to be measured which would require that holes be drilled in the surface at those specific points. This is not only inconvenient in the installation and data collection stages of experimentation, but not possible in flight testing because invasive alterations of the aircraft's surface is not desirable and typically not allowed. Because of this, the new prototype skin friction probe must be minimally invasive to the surface and allow for a direct measurement of this disturbed pressure reading without necessitating a true wall static tap.

Another issue that a traditional Stanton device presents for the BLDS device is the issue of having to measure not only the disturbed wall static pressure, but also the undisturbed wall static pressure from the same wall static tap. Naturally, this would be difficult and at some points impossible to do during testing because each and every test point would have to be run twice in order to get that data; once with the razor blade installed, and once with the blade absent from the surface. In order to remedy this, a specific type of freestanding static pressure probe, a Sproston-Göksel probe, was evaluated for its ability to measure a pressure that would be equivalent to that of a true

wall static pressure tap reading. This probe would read the undisturbed static pressure and the Stanton-type device would read the disturbed static pressure. This configuration of probes would allow for a simultaneous reading of both the disturbed wall static tap and the undisturbed wall static pressure reading needed to make skin friction calculations using the Stanton method.

2. TRADITIONAL STANTON GAUGE TESTING

2.1 Fabrication

A Stanton gauge of the traditional geometry was fabricated and tested as an initial proof of concept for the project. To begin the fabrication process a 0.004 inch nominally thick double-edged, stainless steel, commercial razor blade (see Figure 2-1) was obtained and cut to an appropriate size for testing. The final blade dimensions measured 0.40 inches parallel to the blade edge by 0.25 inches perpendicular to the blade edge and the thickness of the blade was measured to be 0.0035 ± 0.0001 inches using a precision micrometer. Since the razor has a double-edged blade, the overall blade thickness of 0.0035 inches serves as twice the effective height for the calibration equations, or 2h.

Figure 2-1. Double-edged 0.004 inch thick commercial razor blade

Cutting the stainless steel blade proved to be somewhat difficult as the cutting process must leave no burrs or distortion to the blade itself. Such surface defects would cause the blade to sit unevenly on the surface and present a non-uniformity in the blade height that would cause the resulting data to be incorrect. Various methods of cutting the

blade were attempted including scissors, tin snips, a high-speed cut-off wheel and finally a CNC laser which provided a clean, burr-free edge on the blade itself.

In addition to the blade fabrication, two wall static pressure ports with a diameter of 0.020 inch were installed in a 2 foot by 3 foot Aluminum flat plate. The location of the installation was 28 inches downstream of the leading edge of the flat plate and 2 inches on either side of the centerline of the flat plate itself. Having two wall static taps would allow for a simultaneous measurement of a disturbed and an undisturbed pressure reading which is required of the Stanton method itself. A trip wire with a diameter of 0.020 inch was installed 3 inches downstream of the leading edge of the flat plate to ensure that the flow regime at the test site 28 inches downstream would be turbulent.

2.2 Installation and Testing

The blade was adhered to the surface of the flat plate using Duco cement which was diluted with a small amount of acetone in order to make it more fluid for easier application. A hypodermic needle was used to apply the cement to the blade in order to ensure a more precise and controlled placement. The leading edge of the razor blade was positioned over the right most static port in the flat plate such that it was aligned between the front edge and the centerline of the hole itself as shown in Figure 2-2.

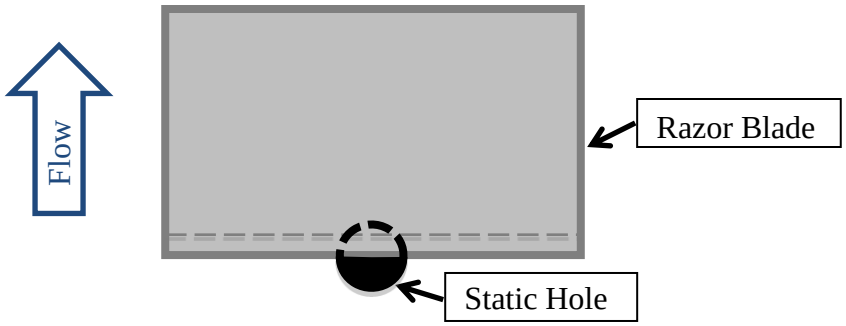

Figure 2-2. Razor blade alignment over wall static port

In order to have a baseline reference skin friction reading at the various conditions that were to be tested, a traditional Preston tube with an outside diameter of d = 0.032 inches was installed on the flat plate at the centerline at the same streamwise location of 28 inches. This Preston tube remained installed and collected data during every experiment. Additionally, Clauser data was provided by Hon Li in his thesis [11] for this particular flat plate from both the hotwire method as well as the Pitot tube method and these results were used as an additional reference for the skin friction measurements. The Clauser data provided can be seen in Appendix B.

After the razor blade and Preston tube were installed on the flat plate, the plate was placed in the test section of the California Polytechnic State University Mechanical Engineering Department's 2 foot by 2 foot wind tunnel. There were five different speeds used during testing for this segment ranging from approximately 20 to 45 meters per second. These speeds correspond to the 20, 30, 40, 50 and 60 Hz settings on the wind tunnel itself. All of the pressure measurements made during the course of the project were made using a Setra Model 239 high accuracy, low-differential pressure transducer. The resulting skin friction coefficients can be seen in Figure 2-3 below.

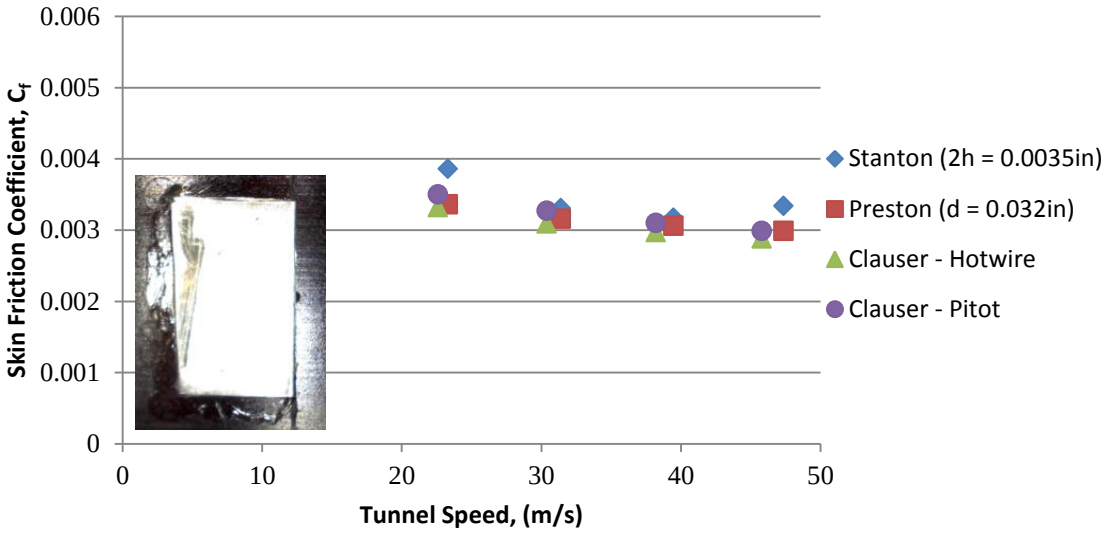

Figure 2-3. Skin friction coefficients vs. wind speed for traditional Stanton gauge with 2h = 0.0035 inch in turbulent flow

As seen in the resulting skin friction values from testing in a turbulent flow regime, the traditional Stanton gauge provided fairly accurate skin friction coefficient values when compared to both the Preston and Clauser data. It is noted that at both the high and low extremes of the speeds tested, the error in the skin friction coefficients is a little higher than that of the mid-speed values.

After the initial gathering of data with a true Stanton gauge, there were a couple of concerns that arose when considering the magnitude of the pressure signals coming from the Stanton device itself. It was noted that the pressure signals from the traditional Stanton gauge are a lot lower relative to those of the Preston tube. It is therefore essential that the small signal from the Stanton device is measured as accurately as possible. An investigation into a pressure sensor that operates in a lower range of pressures than what the pressure sensor on the BLDS device measures might be needed in order to ensure accurate skin friction results. It is also critical that the wind-off pressure readings are as

accurate and current as possible during the data collection process. This could entail the possibility of adding a capability to the BLDS device to gather wind-off data in the middle of the testing process as opposed to the current method of using the wind-off data from the beginning of the test.

The next step in the verification process of the traditional Stanton gauge was to collect data under a laminar flow regime. The trip line was removed from the flat plate to ensure that the flow over the flat plate was laminar. The same razor blade previously used for the turbulent flow testing was utilized again, and was re-glued to the surface using the same procedure. The same experimental set up was used as well which includes the Preston tube as a reference skin friction measurement device and the wind tunnel was run at the same wind tunnel speeds as the turbulent testing. The results of this experimental run as well as a picture of the blade cemented in place over the wall static tap can be seen in Figure 2-4 below.

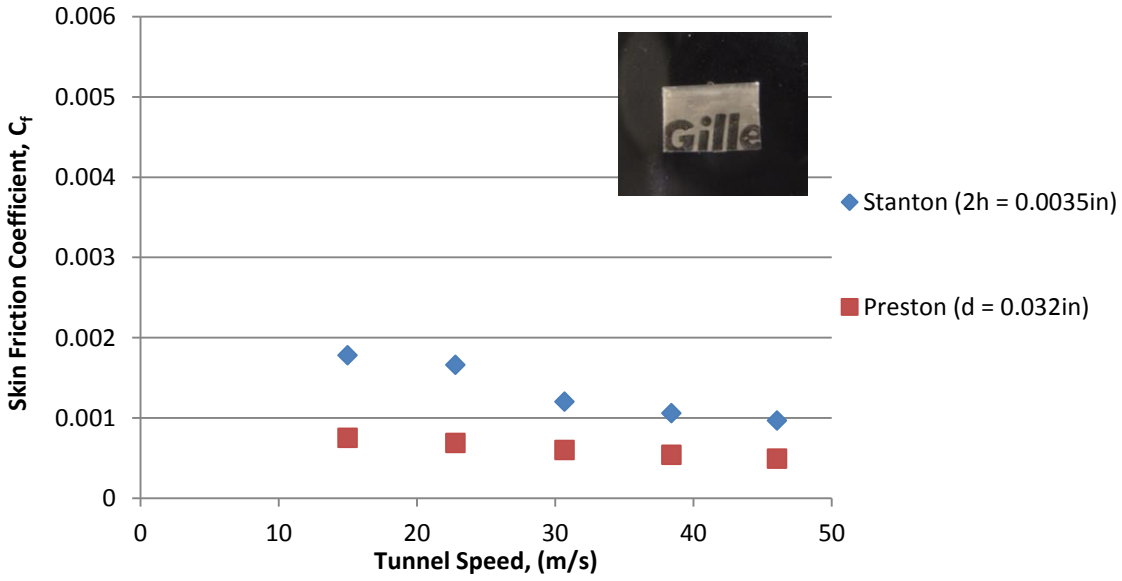

Figure 2-4. Skin friction coefficients vs. wind speed for traditional Stanton gauge with 2h = 0.0035 inch in laminar flow

Overall, the traditional Stanton gauge provided resulting skin friction values consistent with the flow regime and testing conditions and further investigation was done into developing prototypes using this method as a basis.

3. STATIC PRESSURE MEASUREMENT

3.1 Background

Static pressure measurements are required for many different aerodynamic calculations including skin friction measurements. With the Stanton gauge, the surface static pressure has been obtained from a static pressure tap installed in a surface. The surface static pressure tap requires a very small hole, typically 0.02 to 0.04 inches in diameter, to be drilled perpendicular to the surface from which the pressure can be accessed and measured [12]. Depending on the model being investigated, accessing the pressure can be difficult based on certain factors with the model's geometry as well as the circumstances surrounding the testing. A schematic of a generic wall static pressure tap can be seen in Figure 3-1.

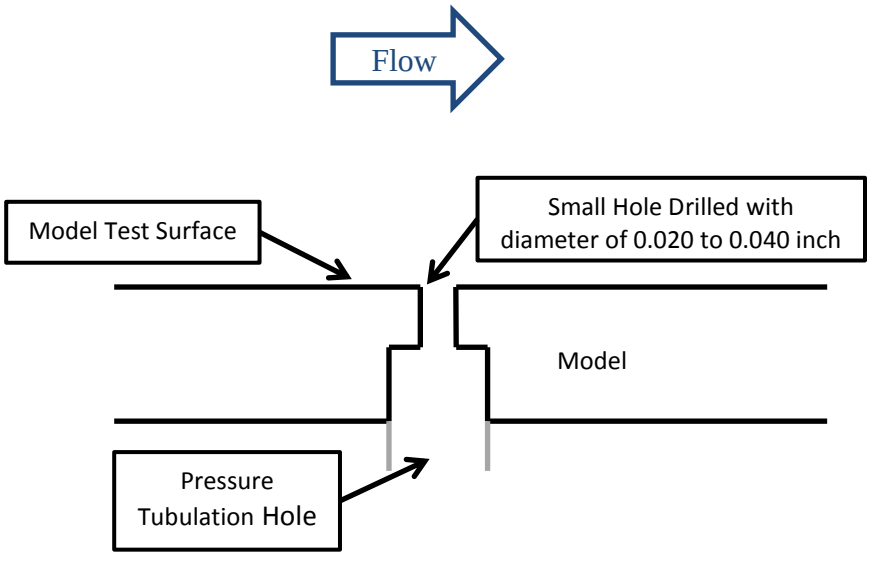

Figure 3-1. Schematic demonstrating a traditional wall static pressure tap

As seen in the figure above, the pressure needs to be accessed on the other side of where the wall pressure tap was drilled. This can be achieved either externally or internally. With relatively thin model surfaces, like the one shown above, the pressure tap can be drilled through the model and the pressure tabulation can be accessed externally on the other side of the model. This method is acceptable only if the other side of the model is not being evaluated and no pressure measurements are being made on that surface. If the opposite side of the model is being evaluated, the pressure can be accessed internally within the model body itself, given that the model is thick enough in this location to accommodate the required equipment.

Another issue arises with using a traditional wall static tap when multiple measurement locations are required during testing. At each location, a wall static tap has to be drilled into the surface to get the appropriate pressure reading for that measurement location but sometimes the locations where the static pressures may be desired is not known until the testing is already underway. It is common that the location of the necessary wall static taps is unknown until preliminary measurements are made to determine locations of interest. At this point, the taps would need to be drilled and the pressure measuring equipment needs to be set up to make the additional pressure measurements.

3.2 Static Pressure Requirement for Stanton Correlation

The ultimate goal of the project is to be able to measure skin friction on an airplane's surface during flight test conditions using the Stanton gauge method. In order to use the Stanton method, a reference wall static pressure measurement must be

available near each measurement location. Under flight-test rules, the BLDS equipment is not allowed to permanently alter the surface of the airplane. With this requirement, having a true wall static pressure tap is unattainable because drilling into the airplane surface would be a permanent alteration. In order to overcome this challenge, the possibility of using a Sproston-Göksel probe to measure wall static pressures was investigated.

Another important issue regarding the use of the Stanton method is the level of accuracy that is required. The pressure readings from Stanton blades are typically on the order of around 5 percent of the reference dynamic pressure. With such a small signal, the uncertainty in this measurement must be kept to a minimum so as to avoid having it make a significant impact upon the readings themselves. When considering this issue with respect to the Sproston Göksel probe, it is important that the static pressure that it is reading is accurate enough to not cause a large error in the pressure reading and subsequently the skin friction value.

3.3 Sproston Göksel Surface Static Probe

J. L. Sproston and Ö. T. Göksel published a paper [13] in 1972 detailing a new method for measuring surface static pressure. Their method utilizes a special probe that sits atop the model surface where the static pressure is measured. This special “surface static tube” is a metal tube with the tip plugged in the shape of a hemisphere and placed into the direction of the flow. Two small static holes are drilled into the surface tube perpendicular to the tube length and parallel to the edge of the tube that would rest on the model surface. The design of the probe is shown in Figure 3-2 below [13].

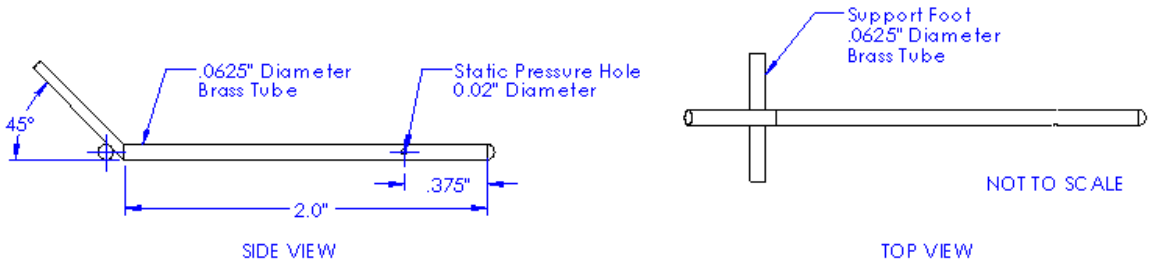

Figure 3-2. Surface static tube design by Sproston and Göksel [13]

These two static holes located in the side of the surface tube allow pressure measurements that closely corresponds to a wall static pressure that would be read from a true wall static tap when the probe axis is aligned with the local surface flow direction [13]. Similar to a regular pressure probe, the pressure measured by the static holes is transmitted through the probe body and a tubulation is connected to the end by which Tygon pressure tubing is connected.

3.4 Testing Results

3.4.1 Sproston and Göksel Probe Testing Completed by Mark Bleazard

The Sproston and Göksel probe was tested on a flat plate with different pressure gradient settings by Mark Bleazard [14] as part of his thesis. The flat plate that was used for testing contained an elliptical leading edge as well as existing wall static taps at the locations to be investigated. Testing was completed using the flat plate under three different scenarios: a favorable pressure gradient (flow acceleration), an adverse pressure gradient (flow deceleration), and no pressure gradient. The testing was done for different

probe yaw angles as well as at different stream-wise locations on the flat plate. In order to evaluate the accuracy of the Sproston-Göksel probe in taking static measurements, it was compared with the true wall static readings using the pressure coefficient, C_P. The coefficient of pressure is a dimensionless value which takes the pressure differential of interest and normalizes it by the reference dynamic pressure of that measurement. The difference between the true wall static and the Sproston-Göksel probe was the differential pressure used in this case. The results of these tests can be seen in Figure 3-3, Figure 3-4, and Figure 3-5 below with the pressure coefficient plotted against the yaw angle for various streamwise locations on the plate as indicated, from [14].

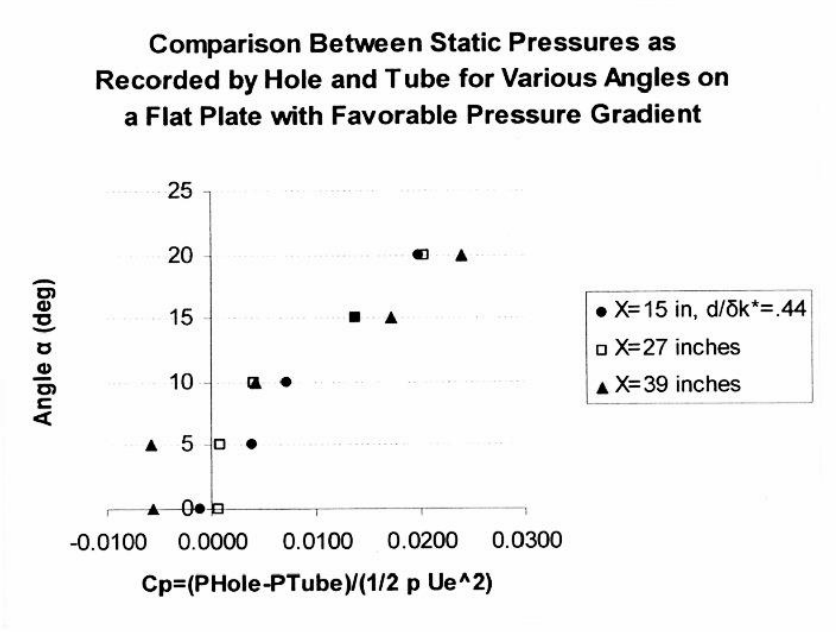

Figure 3-3. Sproston Göksel probe testing for favorable pressure gradient [14]

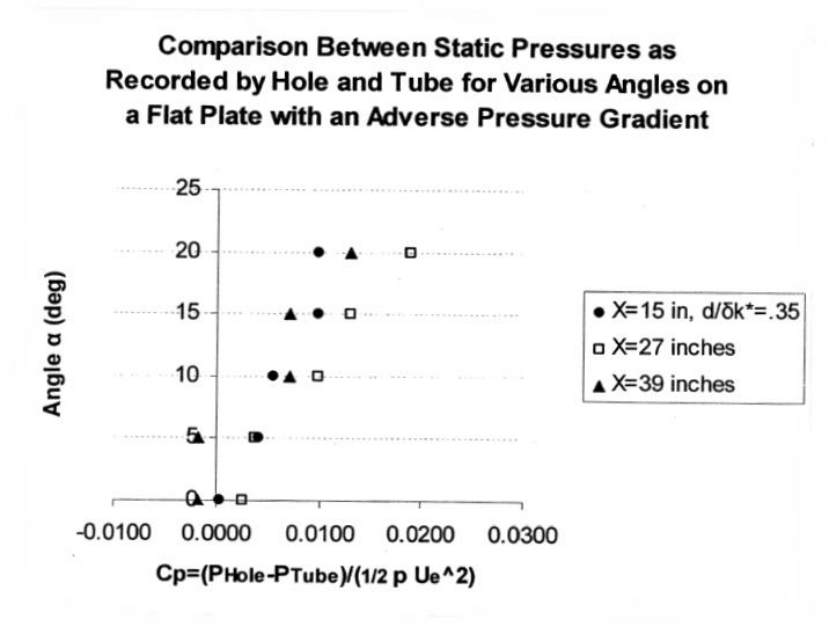

Figure 3-4. Sproston Göksel probe testing for adverse pressure gradient [14]

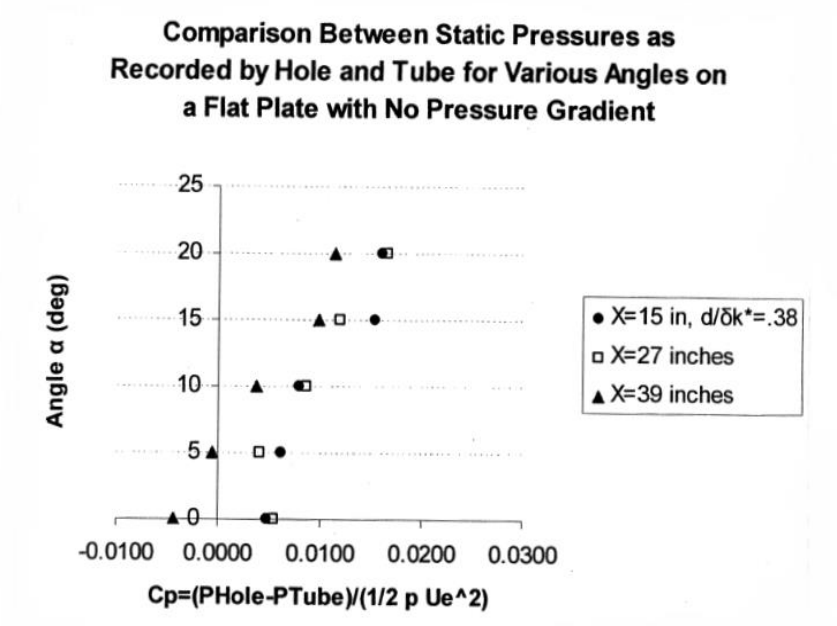

Figure 3-5. Sproston Göksel probe testing with no pressure gradient [14]

As seen with all three cases, the maximum error in the static pressure readings is approximately 2.5 percent of the dynamic reading and it occurs when the alignment of

the probe is within 20 degrees of the local flow direction. The error reduces to 0.5% for probe alignment to within 5 degrees of local flow direction. Overall, the results are very promising with respect to the probe's accuracy in measuring a wall static pressure on a model surface and indicates that the probe can be used to make the static measurements needed for this project as long as the probe's alignment with the local flow direction is within 5 degrees.

3.4.2 Further Testing of the Sproston Göksel Probe

Additional probe testing was completed using the 2 foot by 3 foot flat plate with a slightly favorable pressure gradient in the 2 foot by 2 foot Cal Poly wind tunnel. Two wall static ports with a diameter of 0.020 inches were installed in the plate at 2 inches on either side of centerline and 28 inches downstream of the leading edge to serve as reference values for the Sproston Göksel probe readings. It is important to note that the Sproston Göksel probe used for this testing differs from the original dimensions proposed in 1972. The outer diameter of the probe in this case is 0.042 inch whereas the diameter proposed by Sproston and Göskel was 0.0625 inch. A picture of the experimental set up reflecting the locations and reference names of the wall static measurements as well as the Sproston Göksel probe can be seen in Figure 3-6 below.

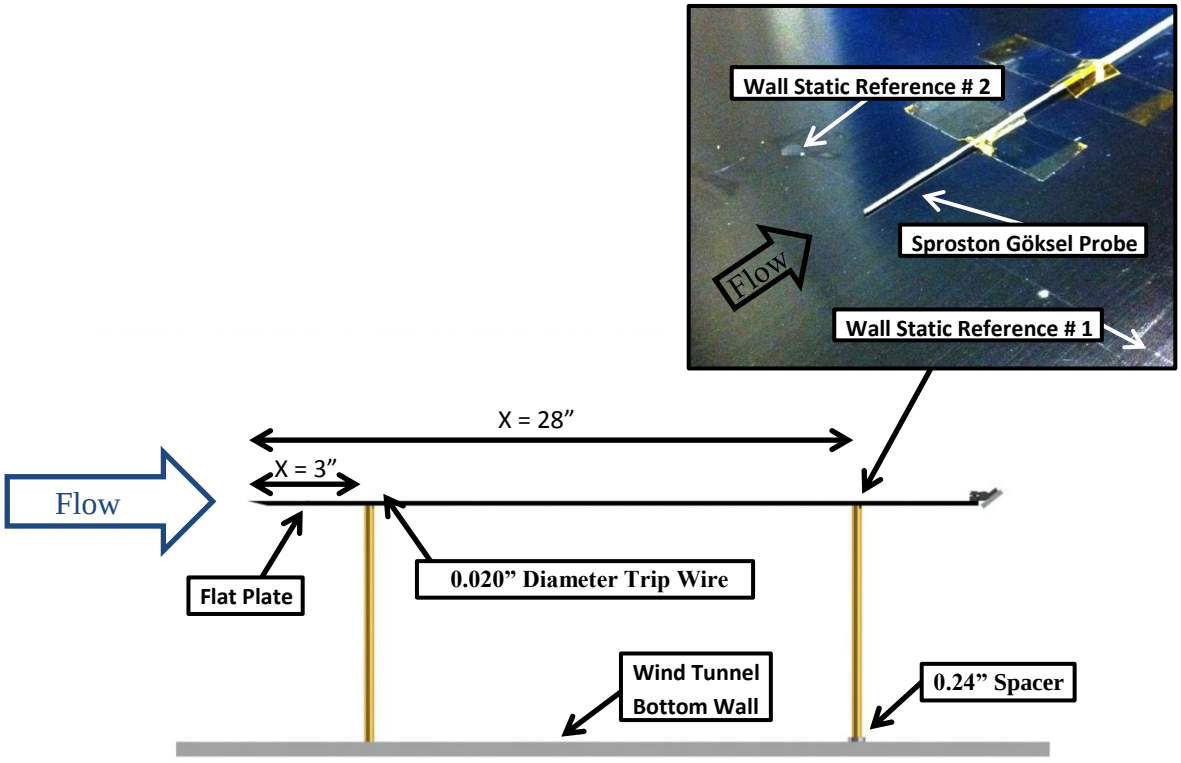

Figure 3-6. Schematic demonstrating overall set up for wind tunnel testing with the flat plate

Measurements were taken under both laminar and turbulent conditions, with the trip line being off and on the plate respectively at various wind speeds in the tunnel and the resulting static pressures from both the probe and the wall static taps were recorded. The differential pressure between the probe and each of the wall static taps was measured and normalized by the reference dynamic pressure to give the coefficient of pressure, C_P. The C_P values were calculated at various speeds for both the laminar and turbulent conditions and can be seen in Figure 3-7 and Figure 3-8, respectively.

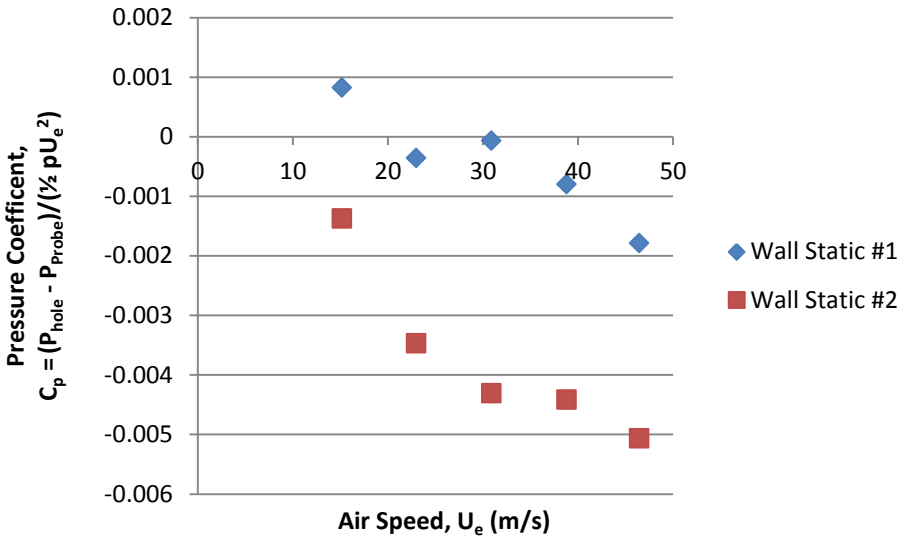

Figure 3-7. Pressure coefficient values vs. wind speed under laminar flow

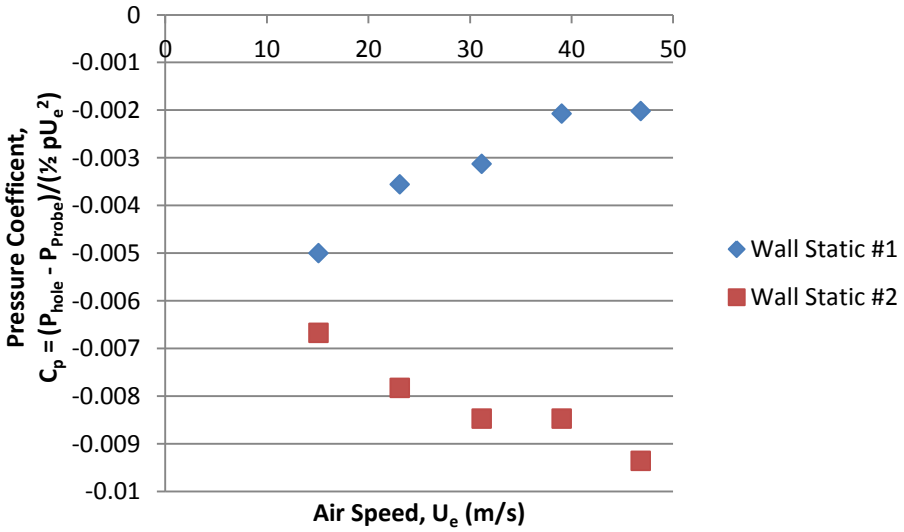

Figure 3-8. Pressure coefficient vs. wind speed under turbulent flow

These results show that the error in the Sproston-Göksel probe is minimal compared to local dynamic pressure measurements with the max error reaching only roughly 1 percent of the reference dynamic pressure. This error is so small that the readings for the Sproston-Göksel probe can be estimated as wall static pressure measurements. This will

allow for the Sproston-Göksel probe to be used in lieu of having a true wall static port which is optimal for the BLDS system requirements.

3.5 Conclusions

In looking at the results from the testing completed by Mark Bleazard [14] as well as recent test data taken in the Cal Poly wind tunnel, it seems as if the 0.042 inch outer diameter Sproston-Göksel probe will suffice in taking the wall reference static pressure measurements required for the Stanton correlation for skin friction. These results prove that the probe not only provides for an easy means of measuring the static pressure but also allows for mobility to measure the static pressure at various locations during the testing. The only requirement that must be met to use the Sproston-Göksel probe in this fashion is that the probe itself must be aligned to within 5 degrees of the flow direction to ensure that the error is kept small.

4. PROTOTYPE DEVELOPMENT

4.1 Initial Prototype Development

In order to overcome the challenges presented by the traditional Stanton gauge, initial concepts for a freestanding Stanton probe that would read the disturbed Stanton pressure without the use of a true wall static tap was proposed. It consists of a razor blade with a hole in the top and a U-shaped shim underneath the razor blade that acts as a spacer. This spacer offsets the blade from the surface and creates a cavity between the bottom of the blade and the top of the model surface. The cavity pressure is accessed by means of the hole in the top of the razor blade, the "static hole". Hypodermic tubing is epoxied over this hole so that the cavity pressure can be fed through the tubing, and eventually through plastic Tygon pressure tubing to connect to a pressure sensor. A schematic of this prototype is shown in Figure 4-1 below.

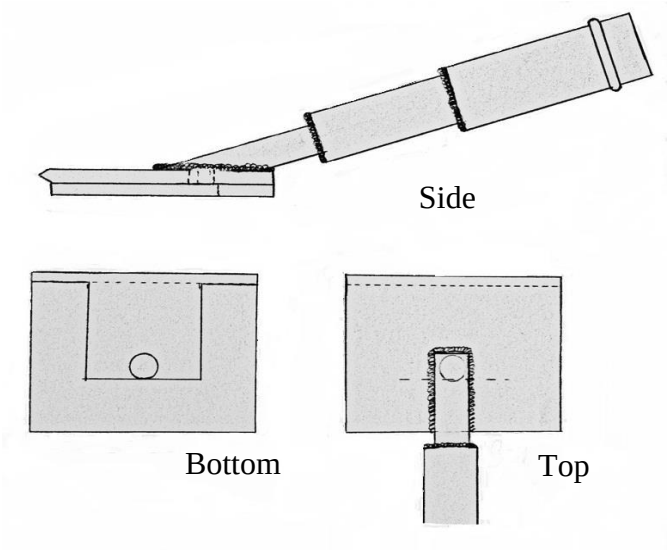

Figure 4-1. Prototype design indicating side, bottom, and top views

Preliminary testing of various minor alterations to the original Stanton design was essential in order to ensure that the prototype design would provide a reading that would be equivalent to that of a true wall static tap. There are three aspects of the initial prototype concept that will be tested: (1) whether an offset or shimmed blade would give the same pressure reading as a blade of the same edge height would give, (2) whether the cavity pressure would give the pressure as a static hole aligned beneath the blade edge, and (3) whether the hypodermic tube atop the blade would alter the disturbed pressure reading. These three elements of the design that contrast with the original traditional Stanton gauge technique are all tested in order to analyze their effect on the pressure reading and ultimately the skin friction coefficient. They will be tested separately as well as together to see the various effects that they have upon the accuracy of the skin friction values. Initially, only the blade offset and the potential tubing obstruction were tested. The results of this testing will provide some initial insight as to whether these certain aspects of the design would be able to provide accurate results. These initial experiments tested the concept only and more detailed testing will be conducted later in the experimentation once the prototype assembly is tested.

4.2 Testing Summary and Code Designations

A short summary of the testing conducted as part of the preliminary investigation into factors of interest to the Stanton assembly can be seen in Table 4-2. This table summarizes the date, description of the experiment, and a code designation for each test completed in this section. These code designations will be used to identify the test itself as well as the individual sensors present during that experiment. The designation code for

each test provide a symbol or a few symbols to indicate the type of sensor being used as well as a number to indicate how many times that individual sensor has been tested. Table 4-1 indicates the meaning of all of the symbols used in the codes.

Table 4-1. Code designation symbol meanings

#S	Traditional Stanton razor blade
#P	Preston tube
#SP	Stanton Prototype
S	Shim spacer
US	U-shaped shim spacer
A	Leading edge aligned with wall static tap
NA	Leading edge not aligned with wall static tap
AO	Angled obstruction
L	Laminar flow regime
T	Turbulent flow regime

Table 4-2. Summary of testing with code designation codes for identification

Date & Figure Number	Description	Designation Code
6/26/13 F. 18	• Stanton blade installed with a 0.004 inch shim spacer at x = 28 inches (h = 0.0059) • Preston tube (D = 0.032 in.) installed at x = 28 inches. • Trip line installed at x = 3 inches to ensure turbulent flow regime	1S-S-1P-T
7/08/13 F. 21	• Stanton blade still installed on flat plate with 0.004 inch shim spacer at x = 28 inches (h = 0.0059 in) • Preston tube (D = 0.032 in.) remains on flat plate surface at x = 28 inches. • Trip line remains installed at x = 3 inches to ensure turbulent flow. • Plugged 0.042 inch hypodermic tubing was taped to the surface above the Stanton blade to present an obstruction to the flow	2S-S-2P-T
7/12/13 F. 25	• The Stanton prototype assembly was installed on the flat plate at x = 28 inches (h = 0.006 in) • No other alterations were made to the previous test's setup and installation	1SP-3P-T
7/17/13	• A Stanton blade was installed over a wall static pressure tap with its leading edge aligned at x = 28	3S-US-A-4P-T

F. 27	inches with a 0.004 inch U shaped spacer underneath the blade body (h = 0.006 in) • No other alterations were made to the previous test's setup and installation	
7/18/13 F. 29	• The Stanton blade and U shaped spacer was removed and reinstalled with the back of its cavity aligned with the existing wall static pressure tap at x = 28 inches (h = 0.006 in) • No other alterations were made to the previous test's setup and installation	4S-US-NA-5P-T
7/18/13 F. 31	• A Stanton blade was removed and reinstalled over a wall static pressure tap with its leading edge aligned at x = 28 inches with a 0.004 inch U shaped spacer underneath the blade body (h = 0.006 in) • An angled obstruction was taped to the surface of the plate over the Stanton blade assembly • No other alterations were made to the previous test's setup and installation	5S-US-A-AO-6P-T
7/22/13 F. 32	• The Stanton blade and U shaped spacer was removed and reinstalled with the back of its cavity aligned with the existing wall static pressure tap at x = 28 inches (h = 0.006 in) • An angled obstruction was taped to the surface of the plate over the Stanton blade assembly • No other alterations were made to the previous test's setup and installation	6S-US-NA-AO-7P-T
7/22/13 F. 34	• Stanton blade and U shaped spacer remained installed with the back of its cavity aligned with the existing wall static pressure tap (h = 0.006 in) • The angled obstruction was removed from the surface of the flat plate • No other alterations were made to the previous test's setup and installation	7S-US-NA-8P-T
7/24/13 F. 35	• Stanton blade and U shaped spacer were removed and reinstalled with the back of its cavity aligned with the existing wall static tap (h = 0.006 in) • No other alterations were made to the previous test's setup and installation	8S-US-NA-9P-T

The corresponding designation code will be listed at the end of the figure title for each plot of the skin friction results from a particular experiment.

4.3 Preliminary Influence Testing

4.3.1 Razor Blade Offset from Surface

The testing presented in this section was conducted to evaluate the use of a shim to offset a razor blade from the surface. In this initial test, the disturbed pressure was measured in the traditional manner, using a surface port. Evaluating whether or not the blade being offset from the surface would create the same pressure as a single-piece blade with the same difference between the surface and the blade edge was the first element to be tested. An additional rectangle with approximately the same dimensions as the original razor blade was cut from the 0.004 inch thick commercial razor blade. This new part acted as a shim spacer to offset the original blade from the flat plate surface. The effective h value would then become the thickness of the shim plus half of the thickness of the razor blade based on the geometry of the parts. Figure 4-2 is a schematic of the assembly that demonstrates the stacking of the original blade on the shim placed underneath. This new geometry was tested in the same fashion as the original Stanton gauge and the resulting skin friction coefficients and a photo of the alignment of the parts can be seen in Figure 4-3.

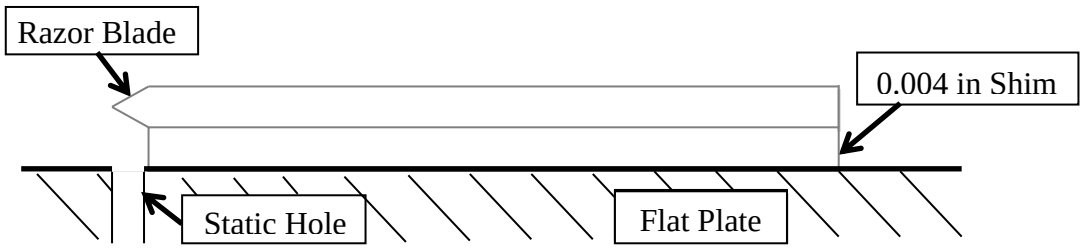

Figure 4-2. Diagram demonstrating the razor blade offset from the surface

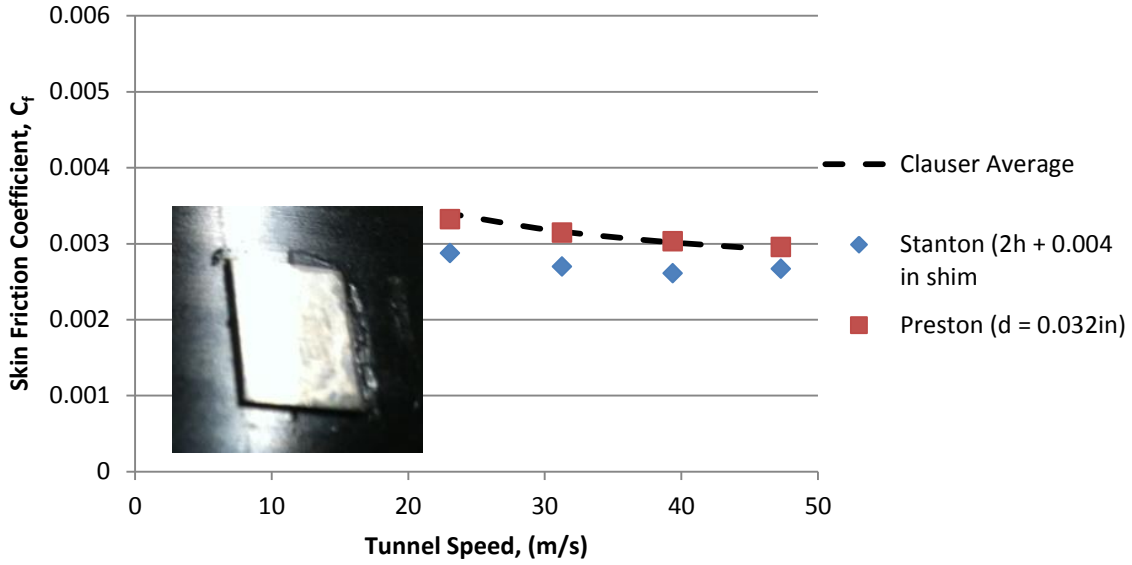

Figure 4-3. Skin friction coefficients at various speeds for a double-sided blade with shim spacer (1S-S-1P-T)

The testing results indicate that the skin friction readings from the configuration with the shim spacer are 10-15% lower than the reference Preston readings. One possible explanation for this result would be potential leakage from around the front corners of the razor blade and shim assembly. This is demonstrated in Figure 4-4 with a top view of the blade and spacer configuration. There could also be some leakage from between the two pieces due to the glue not properly sealing the joint between them. During the installation process, it was difficult to align the two pieces together and subsequently align them to the static hole in the flat plate. This potential misalignment of the two pieces could have also attributed to some of the error in the readings as well.

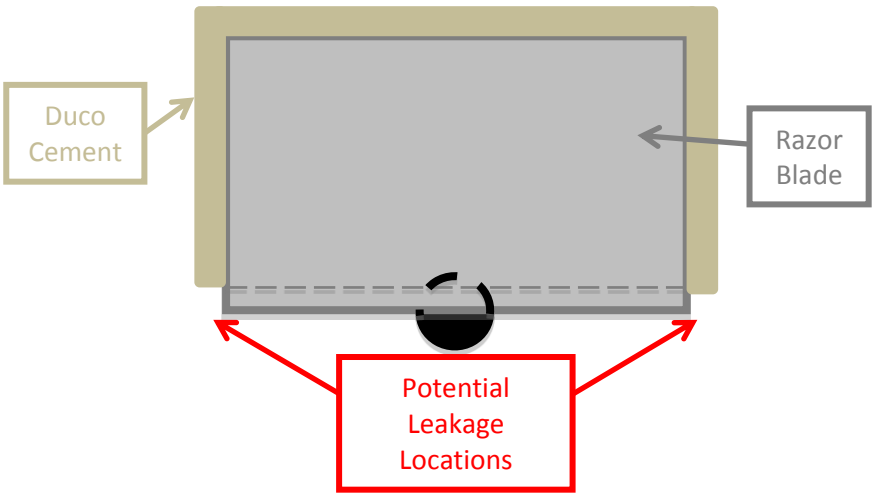

Figure 4-4. Top view of experimental set up indicating potential leakage areas

4.3.2 Hypodermic Tubing Interference Testing

Additional testing was completed to determine whether the downstream obstruction created by the hypodermic tubing atop the blade would alter the disturbed pressure readings from the blade and shim assembly. In order to model this obstruction, a plugged hypodermic tube with an outer diameter of 0.042 inch was taped to the surface of the razor blade slightly downstream of the blade's edge to mimic the geometry of the pressure tubing of the prototype design. The 0.004 inch shim spacer was still glued underneath the razor blade and the alignment remained the same as the previous test. A side view of the assembly demonstrating the orientation of all of the parts can be seen in Figure 4-5. The experimental results can be seen in Figure 4-6 along with a picture of the experimental set up.

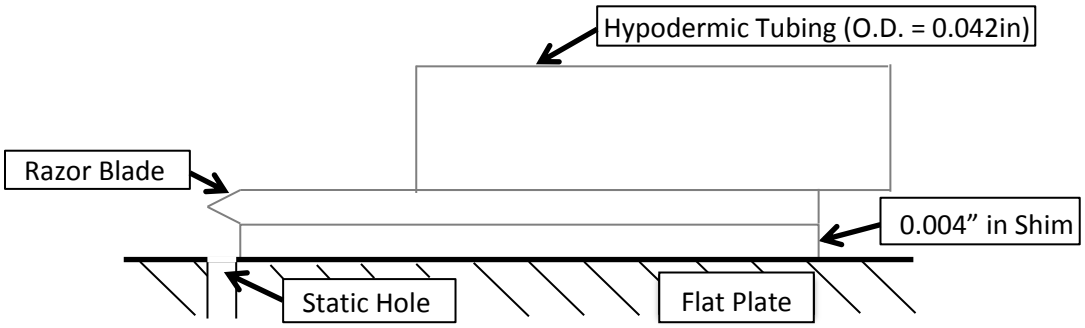

Figure 4-5. Schematic demonstrating the set up for tubing interference testing

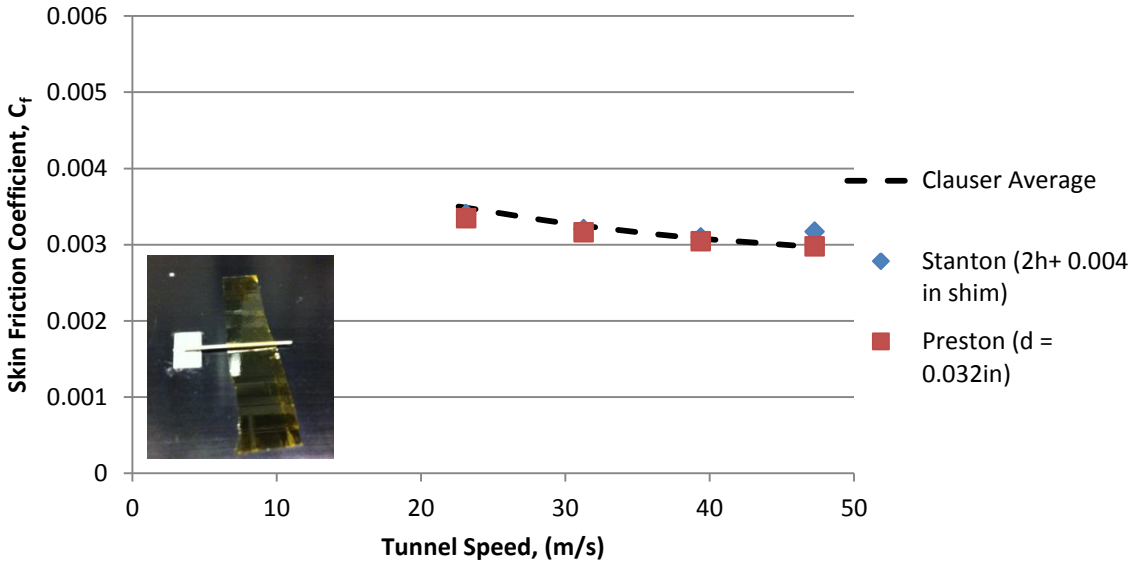

Figure 4-6. Skin friction coefficients at various speeds for Stanton with shim spacer and obstruction (2S-S-2P-T)

The resulting skin friction coefficients from this test agree well with the skin friction values measured using Clauser’s method as well as the Preston tube. When comparing these results with the previously completed testing, both with and without the plugged tubing, it seems as if the obstruction offsets the potential leakage of the previous configuration. It is important to note that while the obstruction accurately represents the

size of the prototype tubing, it does not represent the geometric orientation because the tubing on the prototype will be at some angle with respect to the model surface to be able to connect to the blade pressure. The effect that the angle of the obstruction will have on the readings is examined in subsequent testing once the prototype has been assembled and the angle of the tubing is determined.

4.4 Stanton Prototype Assembly Testing

The prototype assembly was fabricated in an attempt to read an accurate disturbed pressure that a typical Stanton gauge would read without using a surface static port in the flat plate. The prototype utilized a razor blade with a 0.030 inch diameter hole located approximately in the center of the top surface. Instead of a rectangular shim spacer, a U-shaped spacer was made with the same outer dimensions of the razor blade and a width of 0.100 inch all around. The dimensions and geometries of both pieces are shown inFigure 4-7. The razor blade, U-spacer, and model surface together create a very small cavity from which the pressure can be measured through the top hole in the razor blade. Hypodermic tubing with an outer diameter of 0.042 inches and an inner diameter of 0.035 inches was used to access the cavity pressure. This particular tubing was chosen so that the inner dimension was large enough not to obstruct the hole in the blade as well as having the smallest possible outer diameter to create less of an obstruction to the flow. The tubing was ground down at an angle so that this portion of the tube would lay as flat as possible on the surface of the razor blade. This allowed for the prototype to have a less obtrusive profile, so that it would cause less of an obstruction to the flow field.

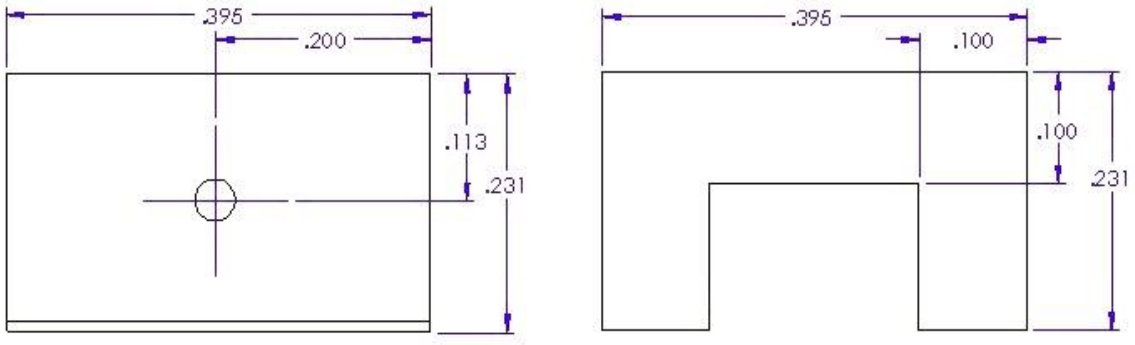

Figure 4-7. Dimensional sketches of the razor blade (left) and U-shaped spacer (right) in inches

The tubing was attached to the razor blade using a small amount of JB Weld epoxy and allowed to cure. Incrementally larger hypodermic tubing was epoxied to the end of the previous tubing in order to eventually attach the tubulation for 1/16th inch Tygon tubing. The angle that the tubing made with the horizontal was approximately 6 degrees after all of the tubing was glued and everything was in place. It was noted that the epoxy joint between the razor blade and the hypodermic tubing was susceptible to fracture because of the small joint and large lever arm that the tubing created. A support foot was therefore created using epoxy in order to help support the fragile joint at the blade. This was accomplished by dripping JB weld epoxy over the hypodermic tubing approximately 1 inch behind the blade and letting it cure atop a piece of Kapton tape as shown in Figure 4-8.

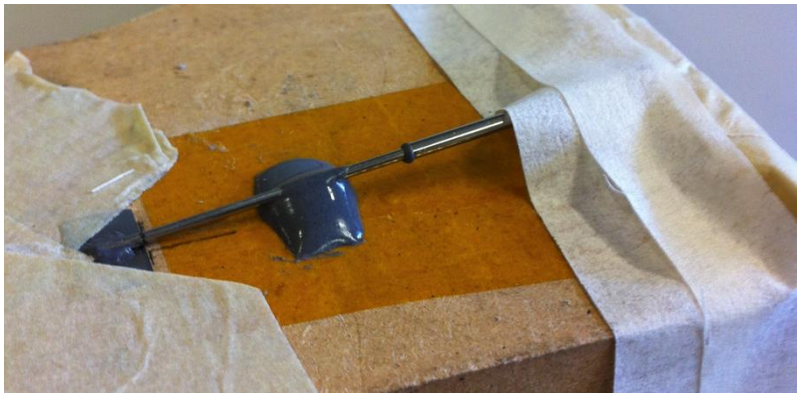

Figure 4-8. Stanton prototype assembly with JB Weld foot 1 inch from the blade

The bottom portion of the assembly was placed on the flat plate 28 inches from the leading edge and the blades were adhered to the surface using diluted Duco cement. A picture of the assembly can be seen in Figure 4-9 below.

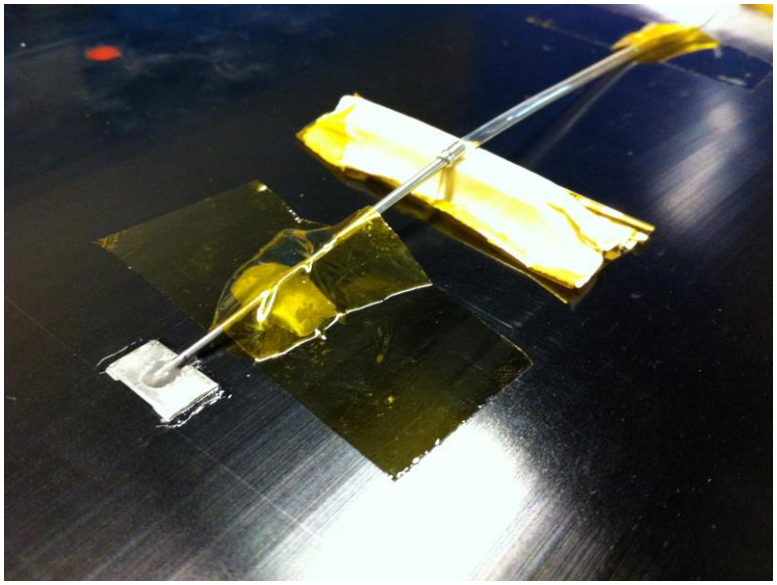

Figure 4-9. Stanton Prototype assembly during installation process

The prototype assembly was tested using the same wind tunnel test speeds as previous experimentation and the resulting skin friction coefficients can be seen in Figure 4-10 below.

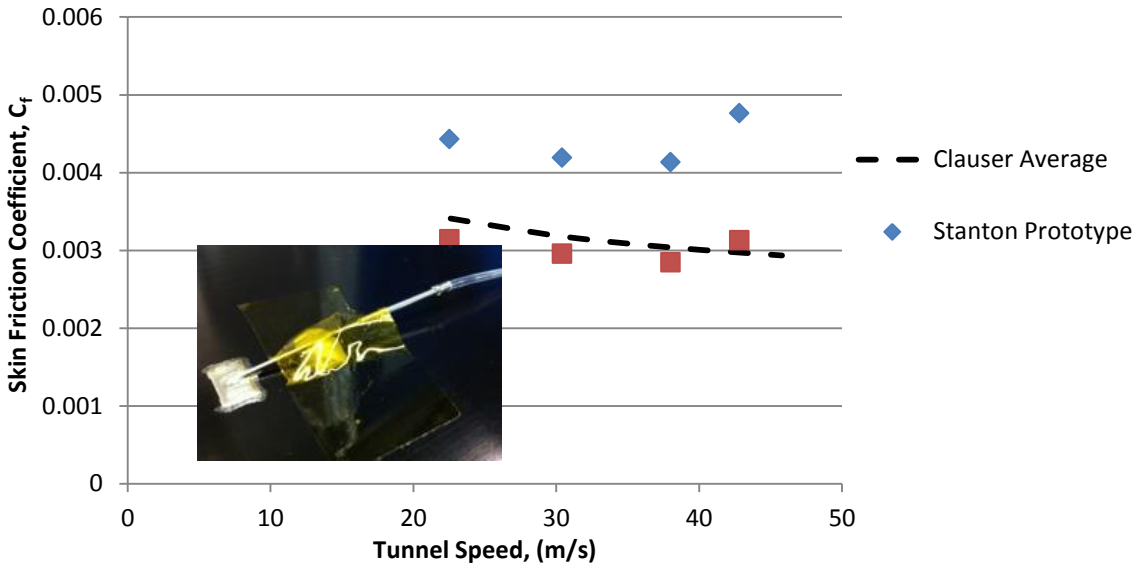

Figure 4-10. Skin friction coefficients for various speeds with the Stanton prototype assembly with turbulent flow (1SP-3P-T)

The skin friction coefficients measured by the Stanton assembly were too high with respect to both sets of reference data. Possible reasons for the error could be the obstruction caused by the angled tubing, as well as the hole location within the cavity. In order to determine if these two components were indeed causing the high readings, additional testing was conducted to isolate each of them and their respective effects on the skin friction. It can be noted that the top speed for the wind tunnel at the time of testing was not the same as the top speed of the wind tunnel when the Clauser data was taken. This was due to the fact that the rear flap on the trailing edge of the flat plate was adjusted to a higher angle with the horizontal between when the Clauser data was taken

and when the current data was being taken. This adjustment caused the upper area of the wind tunnel test section, which is above the flat plate, to decrease causing the air velocity through this area to increase. This discrepancy can be seen in the above figure with the top speeds for the Clauser data being offset from the top speeds for both the Stanton and Preston data.

4.5 Factors Affecting Skin Friction Measurements from Stanton Prototype Assembly

4.5.1 Influence of Hole Alignment with the Razor Blade Edge

In order to isolate the factors contributing to the error in the skin friction measurements by the Stanton Prototype assembly, the geometry of the razor blade and U-shaped spacer was recreated and run separately utilizing an existing wall static port on the flat plate. The leading edge of the razor blade was aligned with the centerline of the static tap to measure the pressure for the first run. A schematic for the set up can be seen in Figure 4-11 and the testing results can be seen in Figure 4-12.

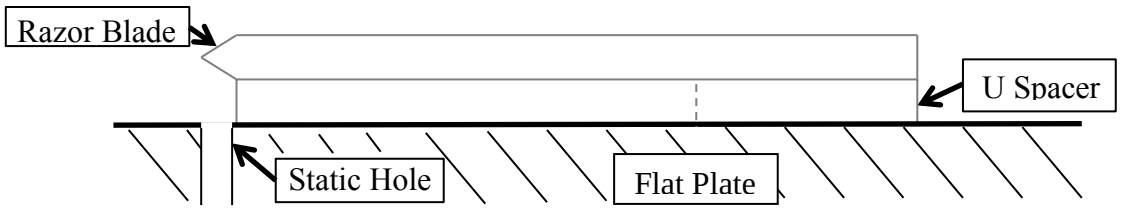

Figure 4-11. Schematic demonstrating blade alignment and experimental set up for hole alignment testing

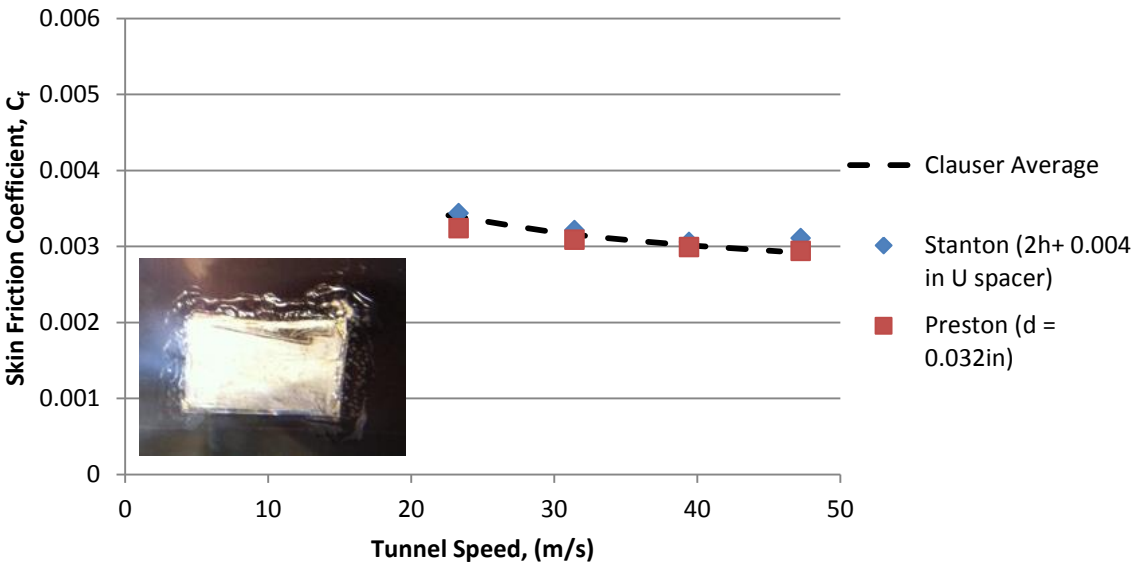

Figure 4-12. Skin friction coefficients for various speeds with the blade and U-Spacer aligned to the front of the static tap (3S-US-A-4P-T)

The results show that U-shaped spacer doesn't have a substantial effect on the skin friction measurements as they agree well with the skin friction values from both the Clauser and Preston data.

The next step was to move the two-piece assembly forward with respect to the static tap in the flat plate so that the hole would lie within the cavity formed underneath the razor blade. The precise alignment was unable to be determined because the hole was underneath the razor blade, but efforts were made to align the hole as far back in the cavity as possible. A diagram representing the alignment of the wall static port within the cavity is shown in Figure 4-13 and the results of the testing can be seen in Figure 4-14.

Figure 4-13. Cut-away diagram demonstrating the location of the wall static port within the cavity

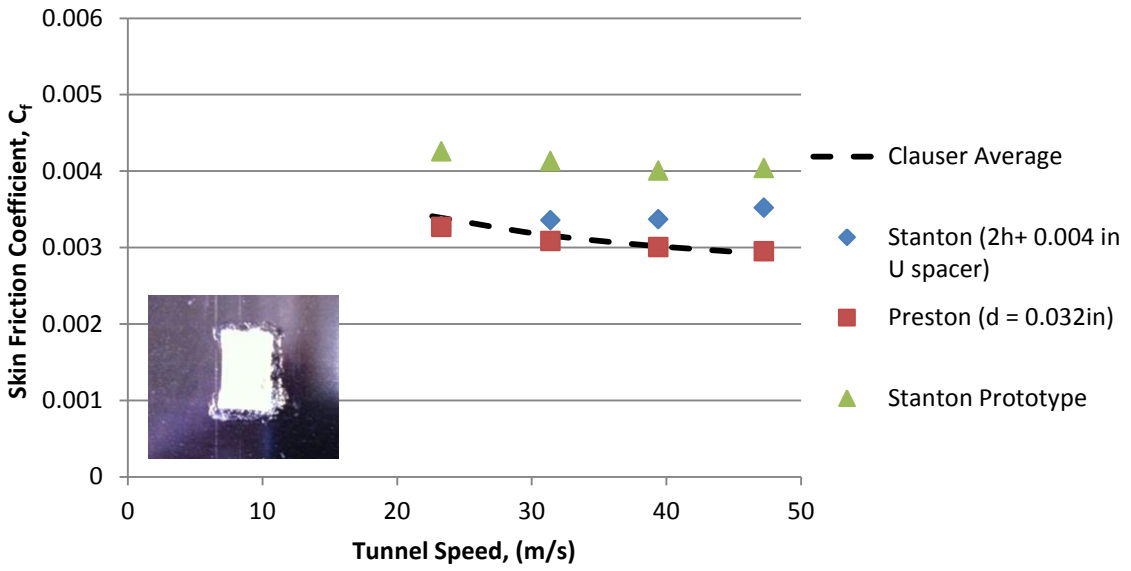

Figure 4-14. Skin friction coefficient vs. wind speed with Stanton blade and U spacer with wall static tap within cavity (4S-US-NA-5P-T)

As demonstrated above, the error caused by the back alignment of the static hole within the cavity does account for some of the total error seen in the prototype assembly. It is interesting to note that as the wind speed increases, the error between the true skin friction coefficient and the measured value increases as well.

4.5.2 Influence of the Hypodermic Pressure Tubing

The next step in isolating the error components of the prototype assembly was to include an angled obstruction along with the blade and spacer configuration which would model the tubing. This was accomplished by shaping a piece of wood to the approximate angle of the prototype assembly and taping it to the surface of the razor blade as shown in Figure 4-15. The alignment of the angled obstruction with respect to the razor blade was closely matched to that of the prototype assembly and the test was run again. The results from this trial can be seen in Figure 4-16.

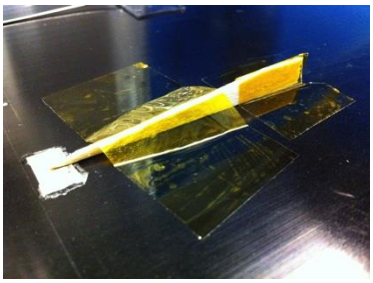

Figure 4-15. Picture of the angled obstruction aligned over the razor blade

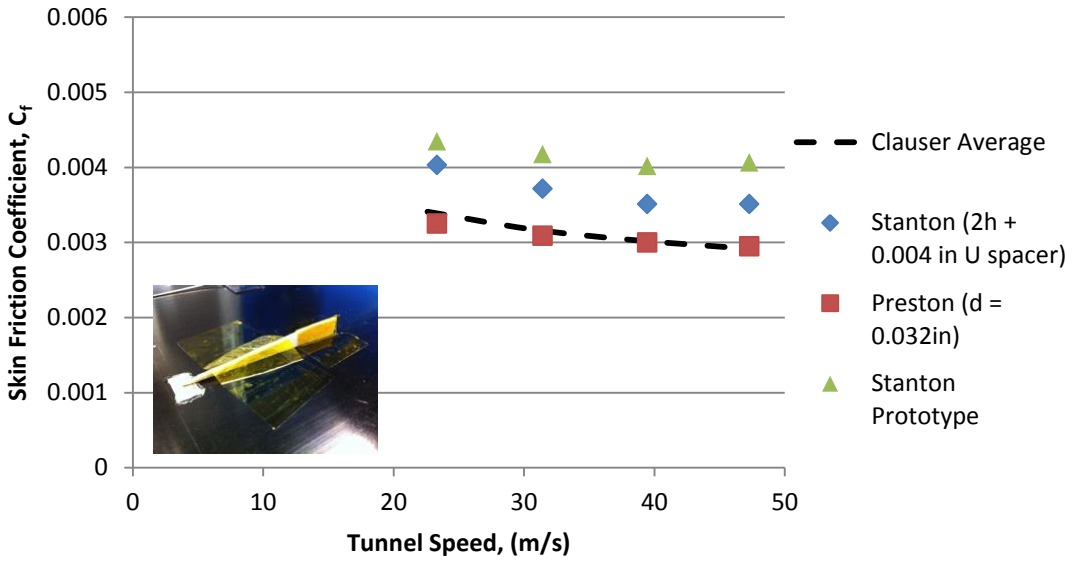

Figure 4-16. Skin friction coefficient for various speeds with razor aligned with the static hole and angled obstruction (5S-US-A-AO-6P-T)

As can be seen with the results above, the angled obstruction has a fairly large effect on the skin friction coefficient and the discrepancy is more prominent at lower wind speeds. This element seems to have the largest impact upon the skin friction measurement out of all of the elements considered for influence testing.

4.5.3 Combined Error Due to Hole Alignment and Angled Obstruction

At this point, it seems as though the combined effect of both the hole alignment within the cavity and the angled obstruction caused by the tubing should result in skin friction coefficients similar to that of the prototype assembly. In order to test this theory, the static hole was aligned to the back portion of the cavity and the angled obstruction was taped down in a similar manner to how the prototype tubing is placed. The

experimental set up as well as the results of testing this configuration can be seen in Figure 4-17.

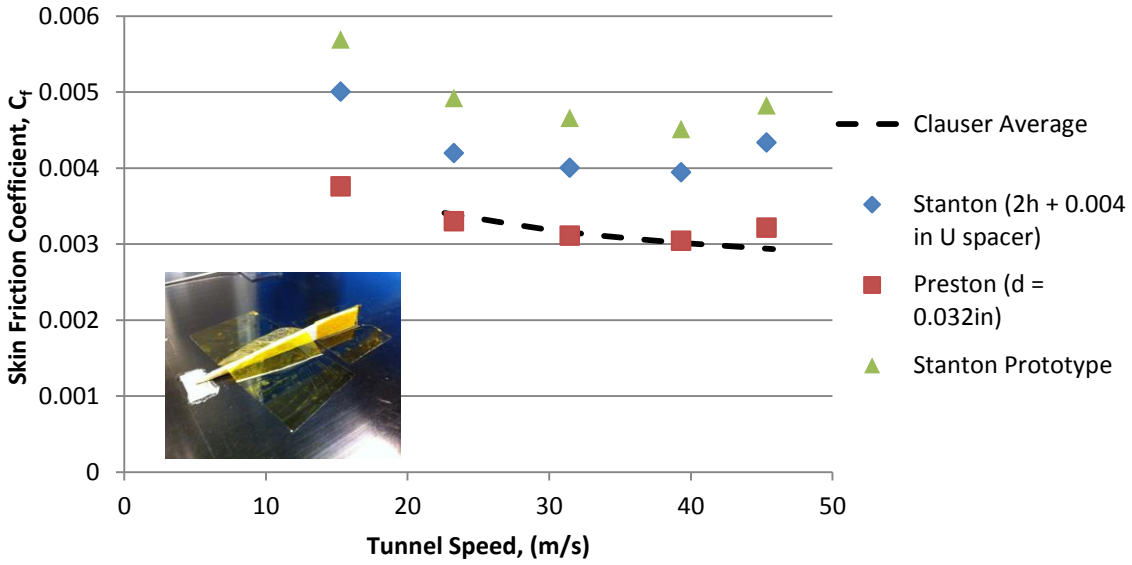

Figure 4-17. Skin friction coefficients at various speeds for wall static port within cavity and angled obstruction (6S-US-NA-AO-7P-T)

As seen in the results of this testing, the combined error of both the angled obstruction as well as the alignment of the static hole within the cavity result in skin friction coefficients that are close to that of the prototype assembly. However, it is important to note that the skin friction values measured by the prototype assembly during this experimental run are significantly higher than previous measurements taken with the same assembly. Since the prototype had not been moved or altered since its initial placement on the flat plate, it is suspected that the adhesive is no longer bonding to the surface causing the prototype to lift up and therefore altering the results. This provided a concern that the assembly might not be able to provide repeatable, accurate results which

would be a very negative attribute of the design. Repeatability testing needed to be conducted in order to determine a proper course of action to remedy the problem.

4.5.4 Repeatability Concerns

In an attempt to gather additional data at lower speeds, previous testing configurations were set up and rerun in the wind tunnel. Noticeable differences between the previously collected data and the current data were observed for identical experimental set ups. As an example, the results for the configuration with a blade and U-spacer with the static hole aligned within the cavity and no obstruction, as shown in Figure 29, are shown in the next few figures. Figure 4-18 demonstrates the first set of data taken with this particular configuration, considered the original data set.

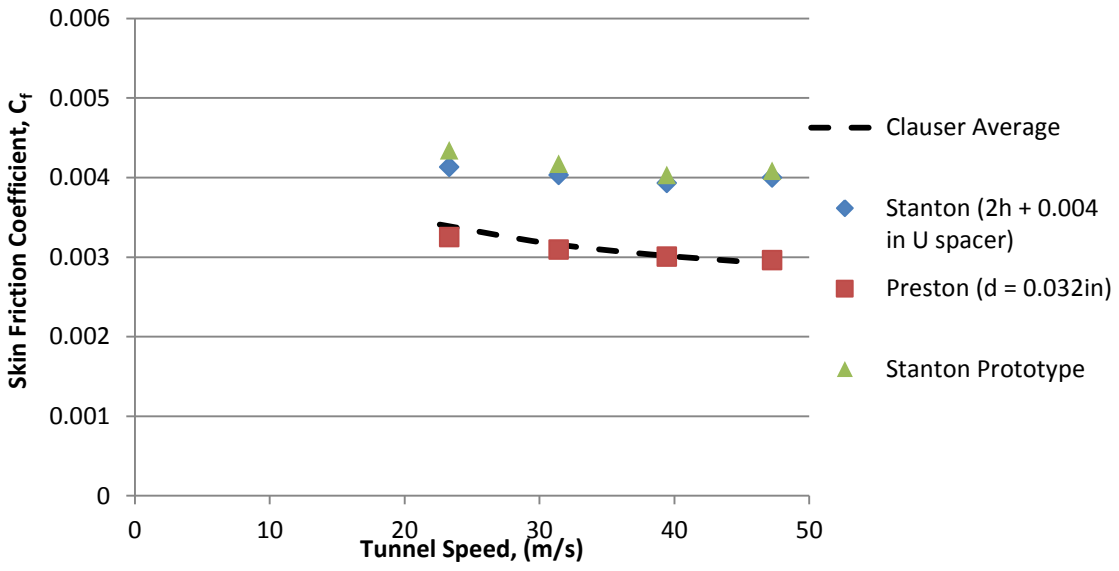

Figure 4-18. Original data with blade and U spacer hole aligned within cavity and no obstruction (4S-US-NA-5P-T)

As shown, the skin friction coefficients from this test are around 0.0035 which are fairly close to the Clauser and Preston tube reference data values. The results from the second testing that was conducted using the same exact set up are shown in Figure 4-19. This data set included an additional data point at a lower wind tunnel speed.

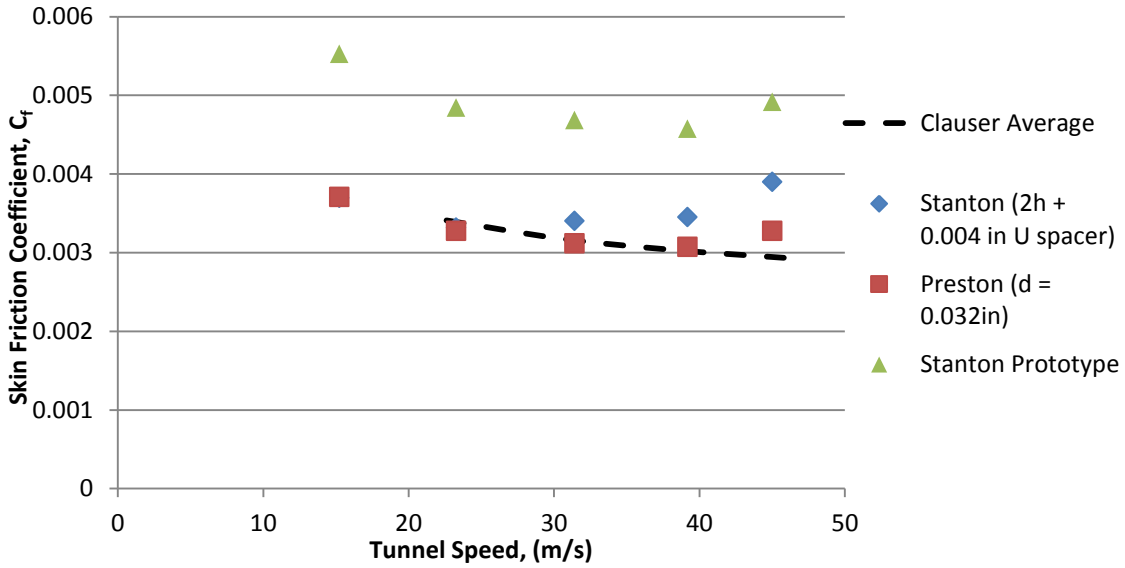

Figure 4-19. First re-trial data for the blade and U spacer with hole aligned in cavity and no obstruction (7S-US-NA-8P-T)

These results gave skin friction values that are a little bit higher than those of the previous data set (Figure 4-18). At the lowest speed tested, the Clauser reference data was not available, but the blade and U-spacer configuration result seems to agree very well with that of the Preston tube data. One possible reason for the increase in skin friction coefficient values could be that the adhesive around the blades had become un-bonded with the surface, allowing the blade to lift up during testing. This seems to be consistent with the results because if this were the case, the blade would lift off the surface further at higher speeds which is consistent with the trend in the data. In an attempt to remedy this

discrepancy, the blade and U spacer were removed from the flat plate and cleaned off. Once the two pieces were re-adhered to the surface, they were allowed to cure and retested in the wind tunnel. The results of this testing can be seen in Figure 4-20.

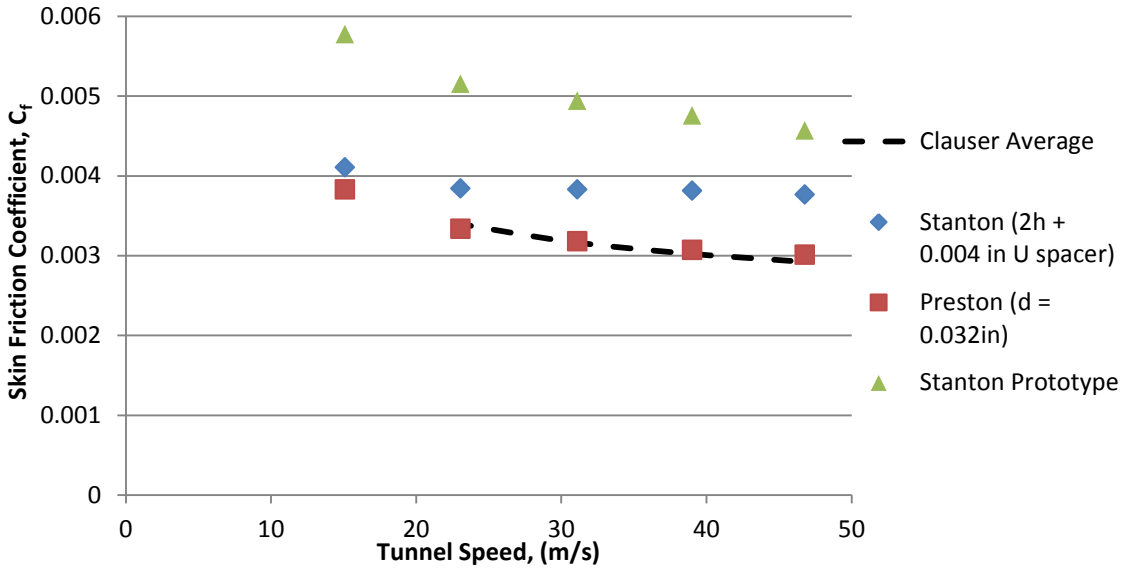

Figure 4-20. Second re-trial of the static hole back aligned and no obstruction configuration after replacement (8S-US-NA-9P-T)

The results of this testing show that even after re-attachment to the model surface, the readings from the blade and spacer configuration are inconsistent with both previous testing results (Figure 4-18 and Figure 4-19). It is important to note that the Stanton prototype results were larger and larger after every test. At the end of the final test, the tape was removed from the prototype and it was noticed that the glue had completely detached from the surface. This could explain the incremental increase in the resulting skin friction coefficient values over time.

4.5.5 Initial Prototype Conclusions

There were some issues encountered with the prototype assembly that will need further consideration and redesigning in order to make the results more acceptable. The main concerns are that the Stanton gauge with the spacer gave results that did not repeat closely, and that the prototype Stanton configuration along with its variations gave inconsistent and non-repeatable results. One possible explanation for these difficulties could be geometric distortion of the blade under wind-on conditions. There could also be thermal considerations due to the fact that the flat plate is made of anodized aluminum and the blades are stainless steel. With a change in temperature, these two materials will expand or contract at different rates possibly causing the adhesive to come off from the surface. Additionally, the issue could just be due to the Duco cement not being strong enough to hold the blade in place consistently. This would allow the blade to deflect from the surface of the flat plate during testing without breaking the cement seal and then return to its original location when the test was over. This lift off from the surface would cause the effective height of the blade to be larger than expected, causing the results to read a lot higher than expected because the effective height used in the calibration equation is a lot lower than the actual effective height during the experimentation.

5. FLOW TAB CONCEPT

A sleek, low-profile pressure measurement probe design patterned after the sharp-edged blade of the Stanton gauge was sought to accurately measure the skin friction on a surface of interest while utilizing the existing Stanton calibrations. The primary requirement for the new device is that it must work without an available surface static pressure tap on the model surface. This requirement arose because the main application of the measurement is to be in flight test, where surface static pressure taps are often unavailable and impractical to install.

The results from the two-piece Stanton gauge prototype for creating the "disturbed" pressure provided some reason for optimism that the current requirements could be met with such a design. However, the two-piece concept proved tedious to fabricate, very difficult to install, and measurement results displayed unacceptable scatter in attempts to get repeatable results. While somewhat encouraging overall, the particular difficulties with the two-piece Stanton gauge design motivated the involvement of Mr. Jim Gerhardt, a senior Cal Poly Mechanical Engineering technician with substantial miniature fabrication experience, in an effort to develop a more practical design.

5.1 Flow Tab Version 1

In collaboration with Mr. Gerhardt, a new design, called a "Flow Tab", was developed which provides the necessary obstruction to generate the "disturbed" pressure reading required for traditional Stanton calibrations without the need for a surface static pressure tap. The main body of the obstruction is formed using a thin (about 0.005 inches

thick), rectangular piece of stainless steel that is machined to form the necessary features of the design. Machining the cavity eliminates the need for a separate U-shaped shim which is a substantial simplification to the design and complexity of the installation process but it does however necessitate highly skilled machining operations. The front of the stainless steel tab has a single sided razor edge ground on the underside to form a sharp leading edge for the incoming flow. A small, shallow cavity only about 0.002 inches deep is machined into the underside of the tab. The pressure within this cavity is communicated through a small hole that connects the cavity to a hypodermic tube that sits inside a channel machined into the top of the tab; the tube is then plumbed to the positive side of a differential pressure sensor whose negative port is connected to a Sproston-Göksel probe. A step is machined into the top surface of the tab so that the front portion of the tab has a thickness of approximately 0.005 inches and the back portion is about 0.020 inches thick. This increase in thickness helps to accommodate and support the hypodermic tubing attached to the top surface of the tab. A picture of the top view of the Version 1 Flow Tab can be seen in Figure 5-1 and a picture of the underside of the tab demonstrating the machined cavity can be seen in Figure 5-2.

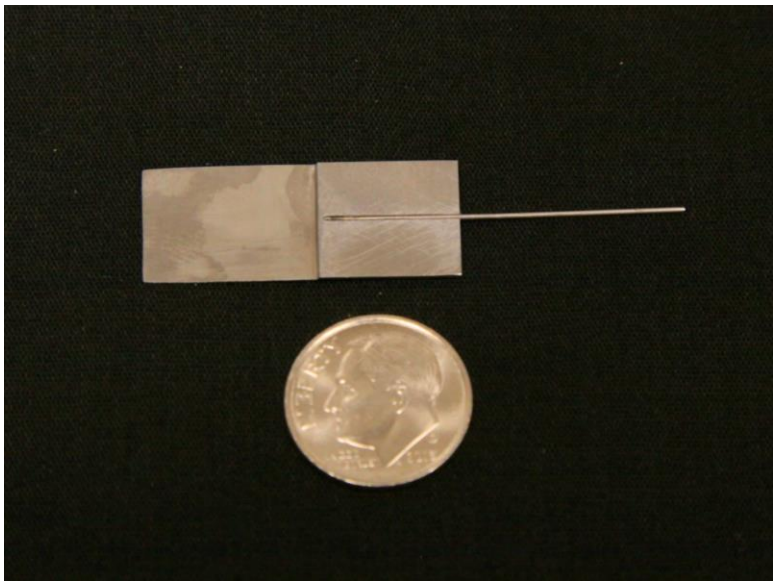

Figure 5-1. A photograph of the initial Flow Tab design (Version 1) along with a dime for scaling.

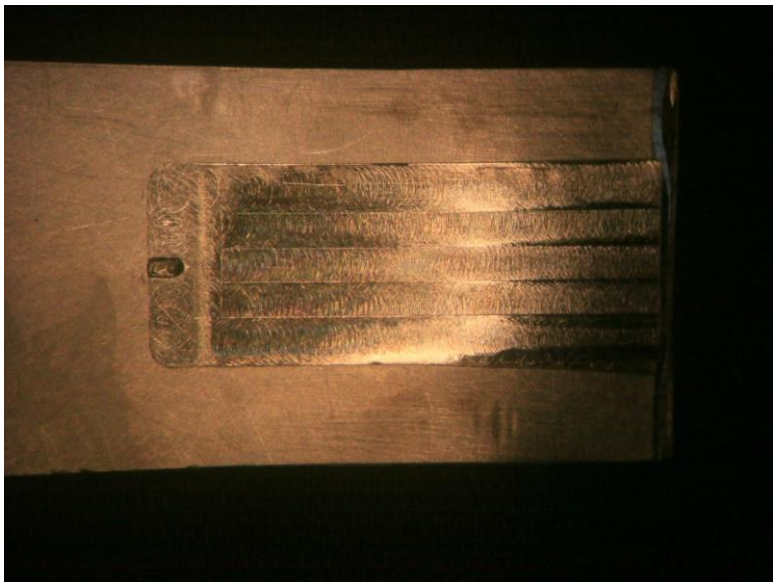

Figure 5-2. A photograph of the underside of the initial Flow Tab design (Version 1)

The tab is adhered to the surface of interest using Duco cement diluted with a small amount of acetone to provide a secure, removable attachment of the tab to the surface and

also to seal the cavity so that there is no leakage of flow from the cavity out the sides or back of the tab body. To install the tab, it's main body is held in place with firm downward pressure using a special block that was machined specially to accommodate the step and tube features on the tab itself. The cement is then applied around the sides and back edge of the tab. The pressure must be maintained until the adhesive hardens to ensure that the adhesive doesn't "wick" underneath the tab perimeter which would cause an uncontrolled increase in the height of the forward edge above the surface. A hypodermic needle is used to ensure precise placement of the adhesive around the edges.

During the fabrication process of the Version 1 Flow Tab, it became apparent that some significant improvements might be possible that would simplify both the fabrication and installation of the device. The result, described in the next section, was a second version of the Flow Tab design.

5.2 Flow Tab Version 2

The Version 1 design required an extensive and time-consuming amount of delicate machining to create the bottom cavity and the step on the top of the thin metal tab body. Both of these machining processes were eliminated with the new Version 2 design. The first change to the Version 1 design was to eliminate the step and position the hypodermic needle directly atop the tab. The hypodermic needle was adhered in place using a silver soldering method by Mr. Gerhardt. A picture of a Flow Tab fabricated using this method of attachment can be seen in Figure 5-3 below.

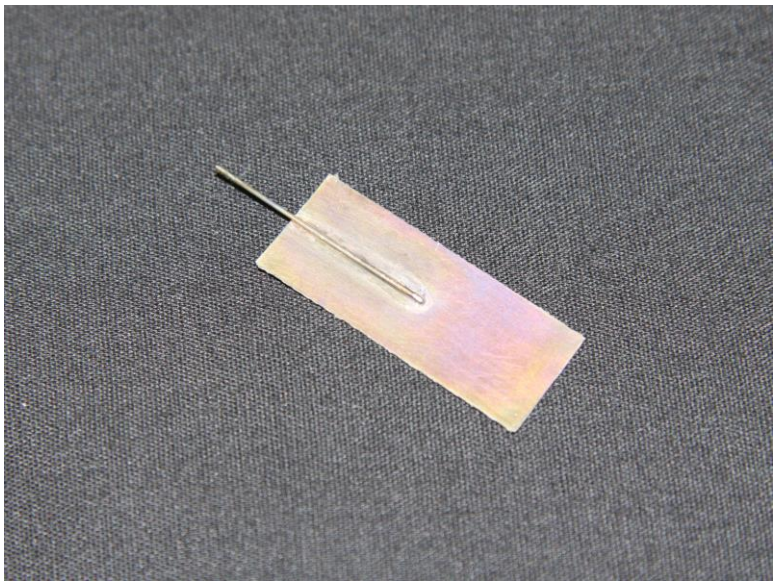

Figure 5-3. Flow Tab fabricated using silver solder to attach the tubing to the body

Later on in the fabrication process a special type of epoxy was found that was capable of reaching extremely low temperatures which would make it suitable for flight testing applications. This epoxy was used in the fabrication of later Flow Tab devices. This change not only eliminated a difficult machining step, it also reduced the profile of the Flow Tab, creating less of an obstruction to the flow.

A second alteration to the Version 1 design was to eliminate the cavity that was previously machined into the underside of the main body. Instead of the machining process, this cavity was created by using 3M F9460PC VHB adhesive transfer tape with a thickness of 0.002 inches cut into the shape of a U. The tape acts as a spacer to displace the main body off of the surface, and the inner part of the U functions as the cavity. Another important advantage of the use of the adhesive transfer tape to create the cavity is that it also functions to attach and seal the Flow Tab to the surface, eliminating the

difficult task of applying the liquid adhesive around the sides and back edge of the tab. A drawing of the Version 2 design can be seen in Figure 5-4 below.

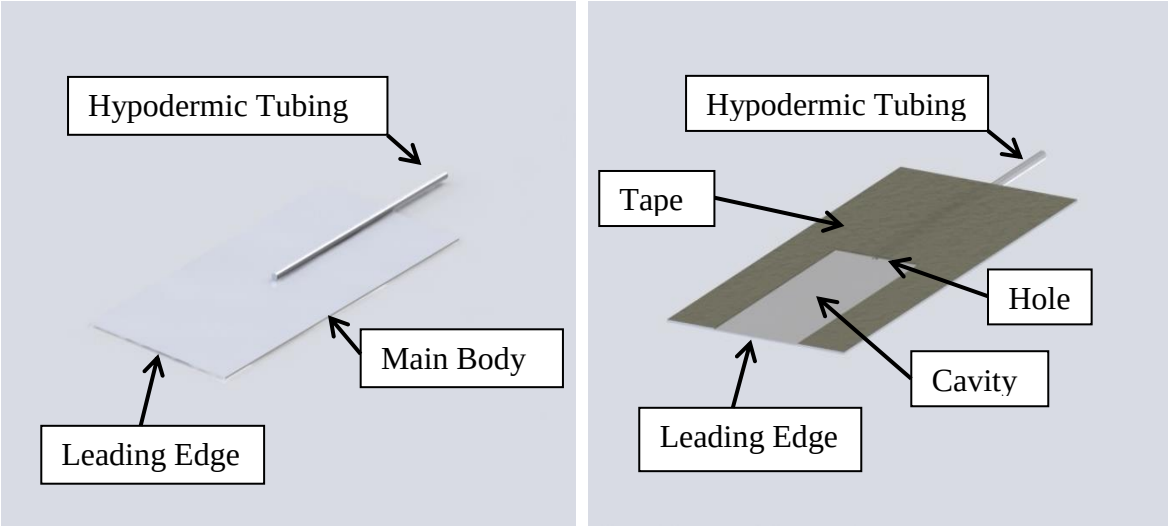

Figure 5-4. Solidworks renderings showing the top (left) and underside (right) of the new design (Version 2)

Stainless steel shim stock of 0.003 inch thickness was used for the main body, so that, including the 0.002 inch thickness of the adhesive, the overall height of the blade edge will be 0.005 inch. The shim stock is easily cut to the required rectangular shape, and the only machining necessary is to drill the hole that connects the cavity to the hypodermic tubing atop the body and grind the sharp edge on the front. This cuts down on the complexity of the fabrication along with the fabrication time required.

5.3 Flow Tab Version 3

The next generation of Flow Tab that was developed was in an attempt to reduce the effective height of the Flow Tab. The bevel of the leading edge of the Flow Tab was

investigated further and two new configurations were developed and tested. Firstly, instead of grinding a single bevel on the underside of the stainless steel shim during the fabrication process, a double bevel was ground into the leading edge of the shim. This would cause the effective height of the Flow Tab to change from 0.005 in to 0.0035 in. The second new configuration was developed with a single bevel ground into the top surface of the Flow Tab body instead of the bottom facing surface. This configuration would allow for the smallest effective height that has been developed of 0.002 in.

5.4 Flow Tabs Identification

A total of 3 prototype Flow Tabs were fabricated, installed, and tested. The first two Flow Tabs were fabricated following the initial design concept, as demonstrated in Figure 34, and have been designated as Version 1 Flow Tabs. The first of those two Flow Tabs to be fabricated and tested is referred to as Version 1 Serial 1 (V1S1); the second Flow Tab that was fabricated and tested that was also based on the initial design is referred to as Version 1 Serial 2 (V1S2). The third Flow Tab was fabricated after the redesign of the Flow Tab concept, as demonstrated in Figure 35, which is designated as a Version 2 Flow Tab. The first and only Flow Tab that was fabricated utilizing this design is referred to as Version 2 Serial 1 (V2S1). The Flow Tabs that were developed with different blade configurations are considered Version 3 Flow Tabs. The double bevel leading edge is referred to as Version 3 Serial 1 Flow Tab (V3S1). The Flow Tab with a single bevel on the top surface is referred to as Version 3 Serial 2 Flow Tab (V3S2). This labeling scheme will be used to identify each Flow Tab as well as label the respective results.

5.5 Testing Results

A short summary of the testing conducted as part of the preliminary investigation into factors of interest to the Stanton assembly can be seen in Table 5-1. This table summarizes the date, description of the experiment, and a code designation for each test completed in this section. These code designations will be used to identify the test itself as well as the individual sensors present during that experiment. See Table 4-1 in Chapter 4 for a list of symbol meanings. The Flow Tab sensors themselves are labeled with their respective version and serial numbers.

Table 5-1. Summary of testing and designation codes

Date & Figure Number	Description	Designation Code
9/16/13 F. 41	• The first version Flow Tab was installed on the flat plate at x = 28 inches downstream of the leading edge • Preston tube (D = 0.032 in.) installed at x = 28 inches • Trip line installed at x = 3 inches to ensure turbulent flow regime	1V1S1-10P-T
9/19/13 F. 42	• The experiment from 9/16/13 was rerun with no alterations to the original set up and installation	2V1S1-11P-T
9/19/14 F. 43	• The trip line was removed from the flat plate to collect laminar data from the V1S1 Flow Tab • No other alterations were made to the previous test's setup and installation	3V1S1-12P-L
10/1913 F. 45	• The V1S2 Flow Tab was installed on the flat plate at x = 28 inches downstream of the leading edge • The V1S1 Flow Tab remained installed on the flat plate from previous testing • Preston tube (D = 0.032 in.) installed at x = 28 inches. • Trip line remained uninstalled from the flat plate surface so laminar flow could be achieved	4V1S1-1V1S2-13P-L
10/19/13 F. 46	• The trip line was reinstalled on the flat plate surface at x = 3 inches downstream of the leading edge to ensure turbulent flow • No other alterations were made to the previous test's setup and installation	5V1S1-2V1S2-14P-T
11/9/13	• The V1S1 Flow Tab was removed from the surface and the V2S1 Flow Tab was installed in its place at x = 28 inches	3V1S2-1V2S1-15P-T

F. 48	downstream of the leading edge • The V1S2 Flow Tab remained on the flat plate surface, unaltered from previous testing • No other alterations were made to the previous test's setup and installation	
11/9/13 F. 49	• The trip line was removed from the flat plate to collect laminar data • No other alterations were made to the previous test's setup and installation	4V1S2-2V2S1-16P-L
5/13/14 F. 51	• The V3S1 and V3S2 Flow Tabs were installed on the flat plate at x = 28 inches downstream of the leading edge • Preston tube (D = 0.032 in.) installed at x = 28 inches • Trip line remained uninstalled from the flat plate surface so laminar flow could be achieved	1V3S1-1V3S2-17P-L
5/13/14 F. 52	• The trip line was reinstalled on the flat plate surface at x = 3 inches downstream of the leading edge to ensure turbulent flow • No other alterations were made to the previous test's setup and installation	2V3S1-2V3S2-18P-T

5.5.1 Version 1 Serial 1 Flow Tab Testing (Turbulent)

The Version 1 Serial 1 (V1S1) Flow Tab was initially tested with a turbulent flow regime imposed by having the wire trip installed on the flat plate. For these tests, the surface static pressure reference was obtained from a wall static port as shown in the photograph of the test setup, Figure 5-5. A Preston tube was employed so that its resulting skin friction measurements could be compared to those from the Flow Tab, providing a control on the results. Results from a Clauser analysis of velocity profiles measured earlier this year are also compared to the Flow Tab and Preston tube results for turbulent conditions. The profile measurements were not made for laminar (untripped) conditions.

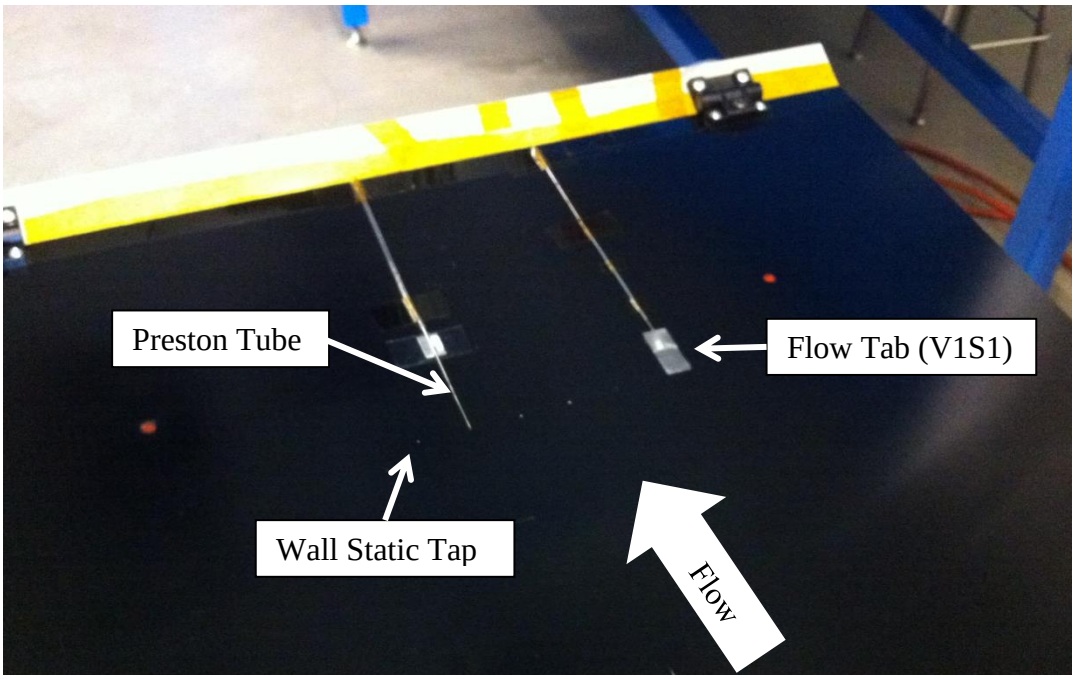

Figure 5-5. Photograph of the test plate showing the setup of the measurement probes

The resulting skin friction values calculated using the pressure readings during this testing are given in Figure 5-6. The Preston tube results are obtained using Preston's calibration, and the Flow Tab results have been computed using East's calibration. Agreement between the Preston and Flow Tab results is well within the desired +/- 5% range, and both agree closely with results from the Clauser analysis of the profiles measured with hotwire and Pitot probes. The only exception is the lowest speed test point, which as noted earlier, does not result in fully turbulent flow and gives scattered results due to the transitional nature of the flow.

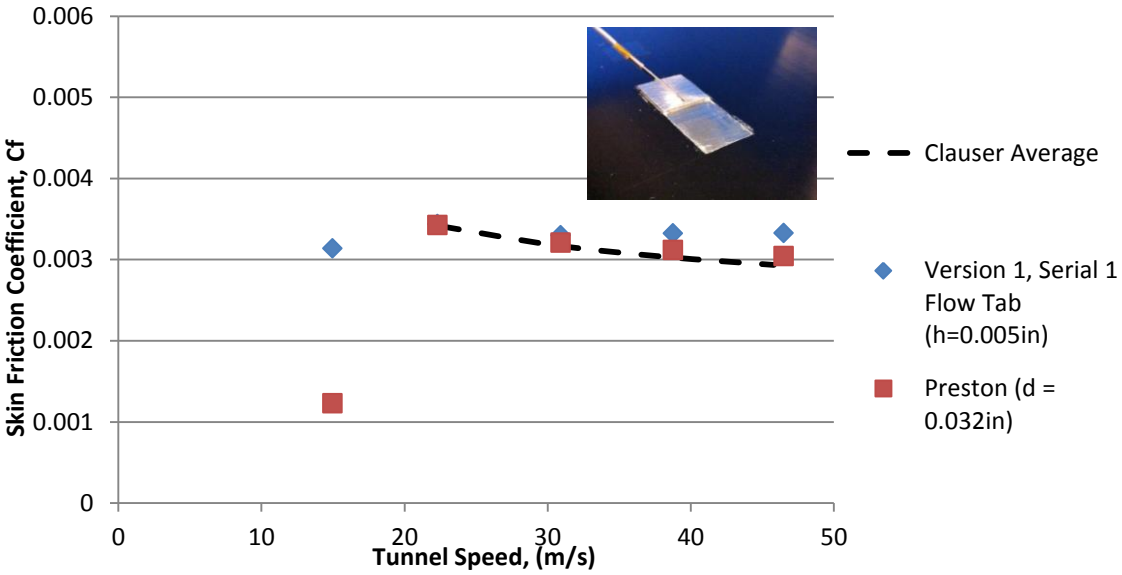

Figure 5-6. Skin friction values at different wind speeds for Version 1 Serial 1 Flow Tab in turbulent flow (1V1S1-10P-T)

5.5.2 Version 1 Serial 1 Flow Tab Retest (Turbulent)

The V1S1 Flow Tab was retested in order to establish repeatability under turbulent flow conditions and the results can be seen in Figure 5-7. It is apparent that good repeatability was obtained.

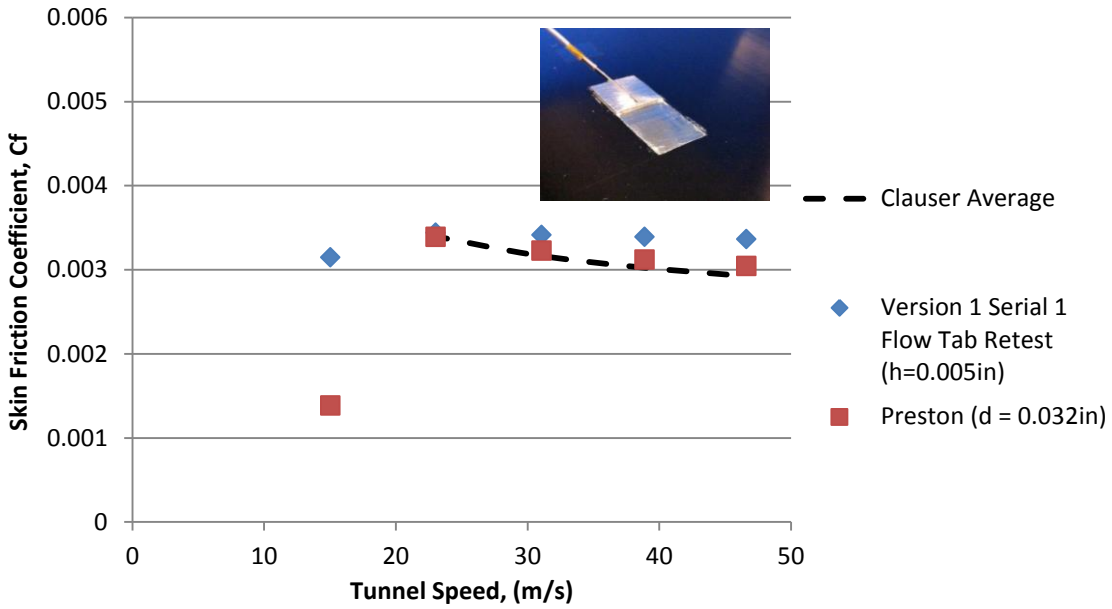

Figure 5-7. Skin friction values at different wind speeds for Version 1 Serial 1 Flow Tab in turbulent flow (2V1S1-11P-T)

5.5.3 Version 1 Serial 1 Flow Tab Testing (Laminar)

The trip wire was removed from the flat plate to establish a laminar boundary layer for testing. The results of the laminar testing of the V1S1 Flow Tab are presented in Figure 5-8.

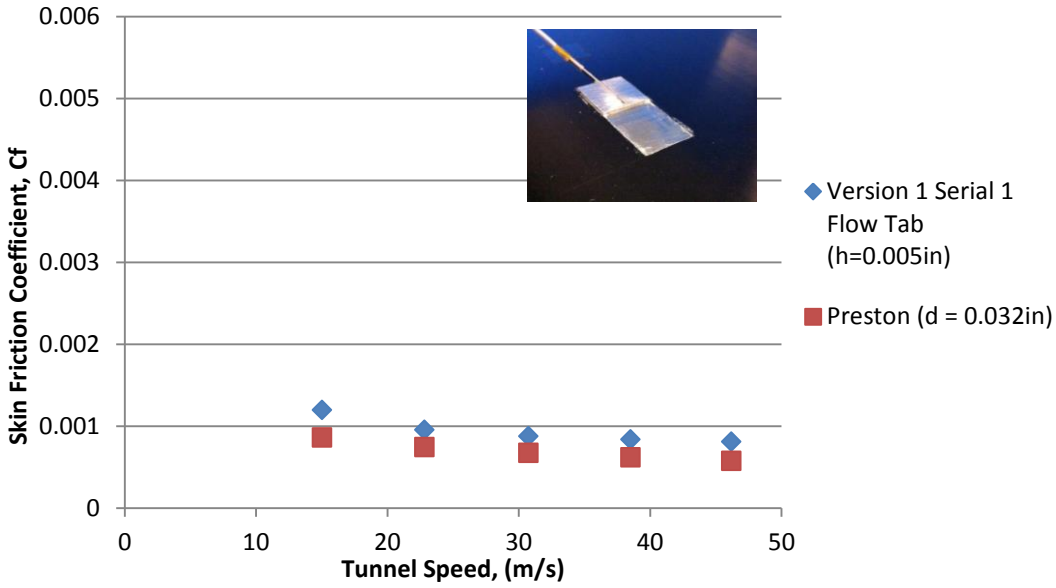

Figure 5-8. Skin friction values at different wind speeds for Version 1 Serial 1 Flow Tab in laminar flow (3V1S1-12P-L)

5.5.4 Version 1 Serial 2 Flow Tab Testing (Laminar)

The second Flow Tab, Flow Tab Version 1 Serial 2, was installed on the flat plate and tested under both laminar and turbulent conditions. For these tests, Flow Tab V1S1 remained installed on the flat plate for further repeatability testing. Figure 5-9 is a photograph showing the respective locations of the Flow Tabs along with the location of the Preston tube and wall static taps. The test results are shown in Figure 5-10; V1S1 and V1S2 are observed to give comparable results which indicates that the fabrication method can give consistent results for the geometry and functionality of the V1 design.

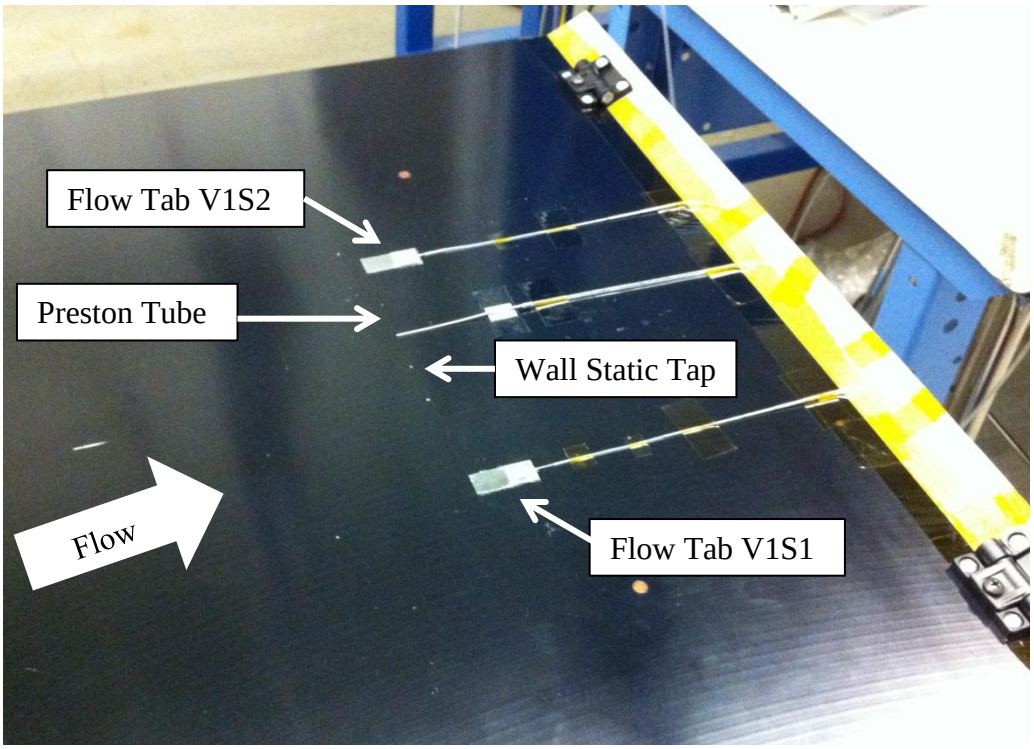

Figure 5-9. Photograph of the flat plate test region demonstrating the location of the equipment

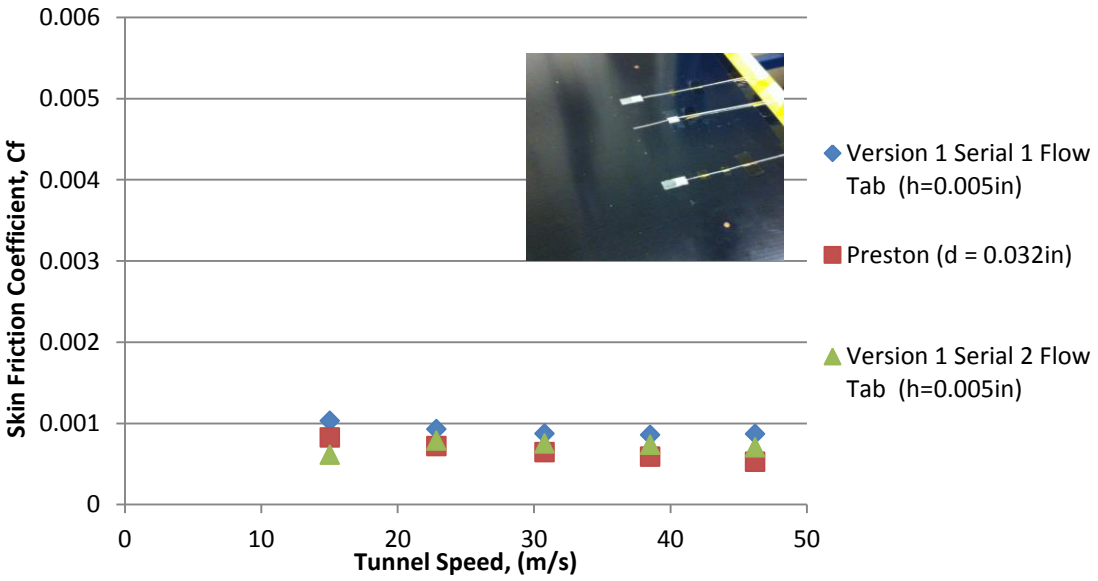

Figure 5-10. Skin friction values at different wind speeds for Version 1 Serial 1 and Serial 2 Flow Tabs in laminar flow (4V1S1-1V1S2-13P-L)

5.5.5 Version 1 Serial 2 Flow Tab Testing (Turbulent)

The trip wire was reinstalled on the flat plate and V1S1 and V1S2 Flow Tabs were tested under conditions identical to those used previously for V1S1. The resulting skin friction values are shown in Figure 5-11. Results for the higher flow speeds were slightly higher than previously measured with V1S1, but agreement with the previous results and the Preston results is still within about 10% which is considered adequate.

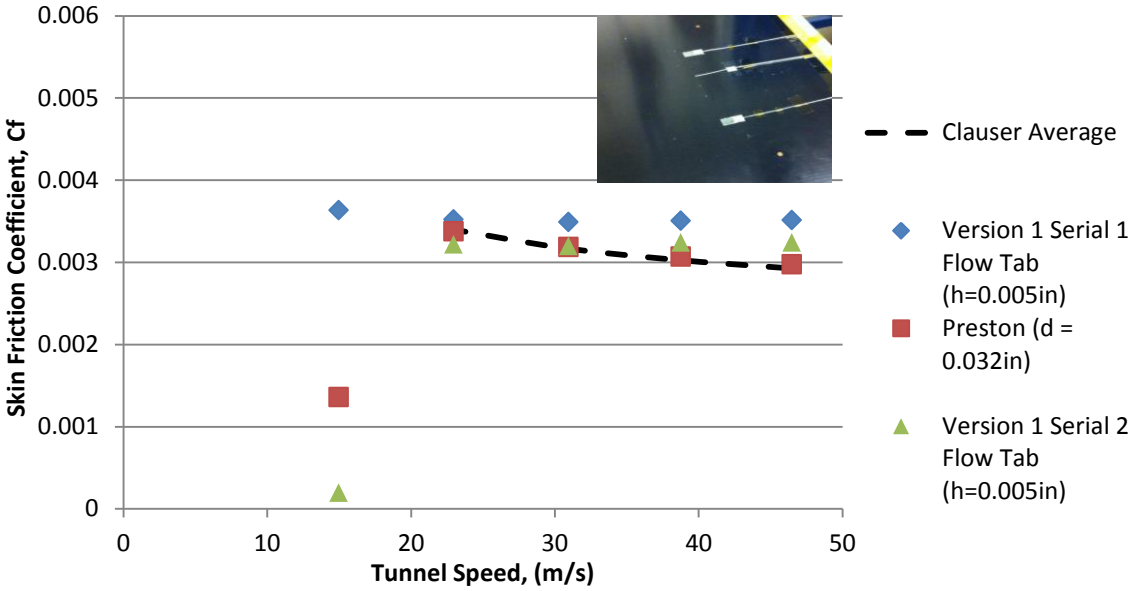

Figure 5-11. Skin friction values for Version 1 Serial 1 and Serial 2 Flow Tabs in turbulent (tripped) flow (5V1S1-2V1S2-14P-T)

5.5.6 Version 2 Serial 1 Flow Tab Testing (Turbulent)

A third Flow Tab, Version 2 Serial 1 Flow Tab, whose design features were described earlier, was fabricated and installed on the flat plate in place of the V1S1 Flow Tab. The trip wire remained in place for this test, giving turbulent flow conditions as employed for earlier testing. The same calibration equations as used for previous turbulent flow tests were also employed for consistency purposes. Figure 5-12 shows

the respective placements of the Flow Tabs as well as the Preston tube and wall static taps. Both V1S2 and V2S1 Flow Tabs were tested and the resulting skin friction coefficient values are plotted in Figure 5-13. The skin friction measurements from V2S1 are observed to agree closely with those from V1S2 and with results from the Preston tube and earlier Clauser measurements.

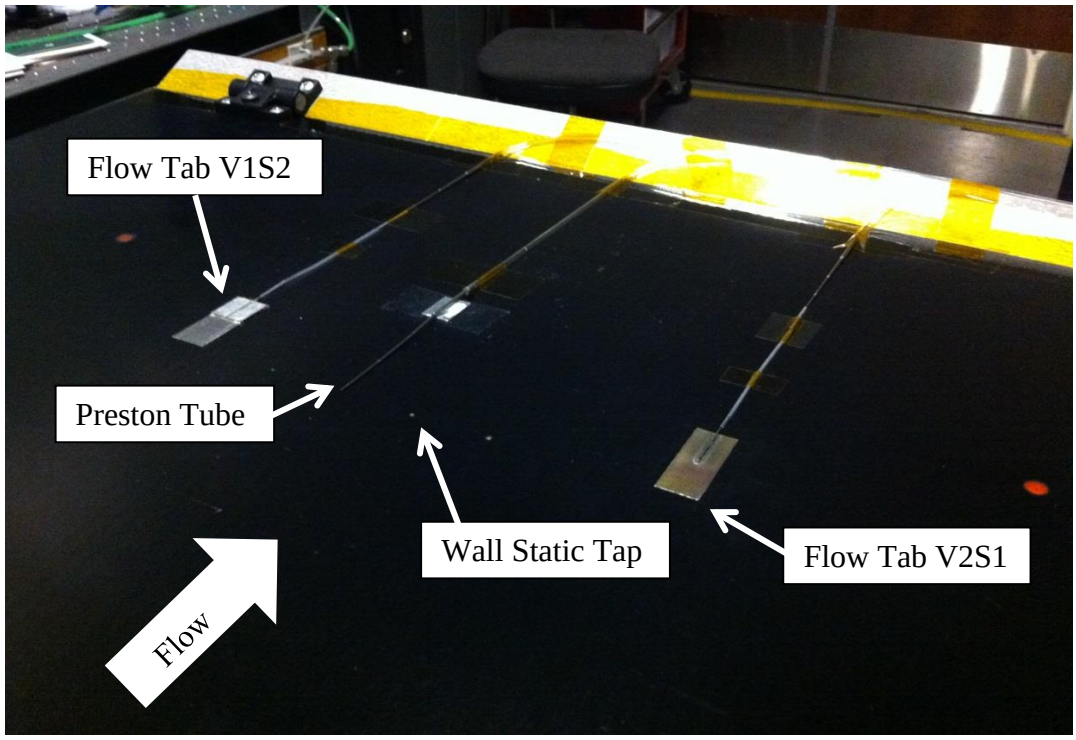

Figure 5-12. Photograph of the test region of the flat plate showing the location of the sensors used for the V2S1 Flow Tab test

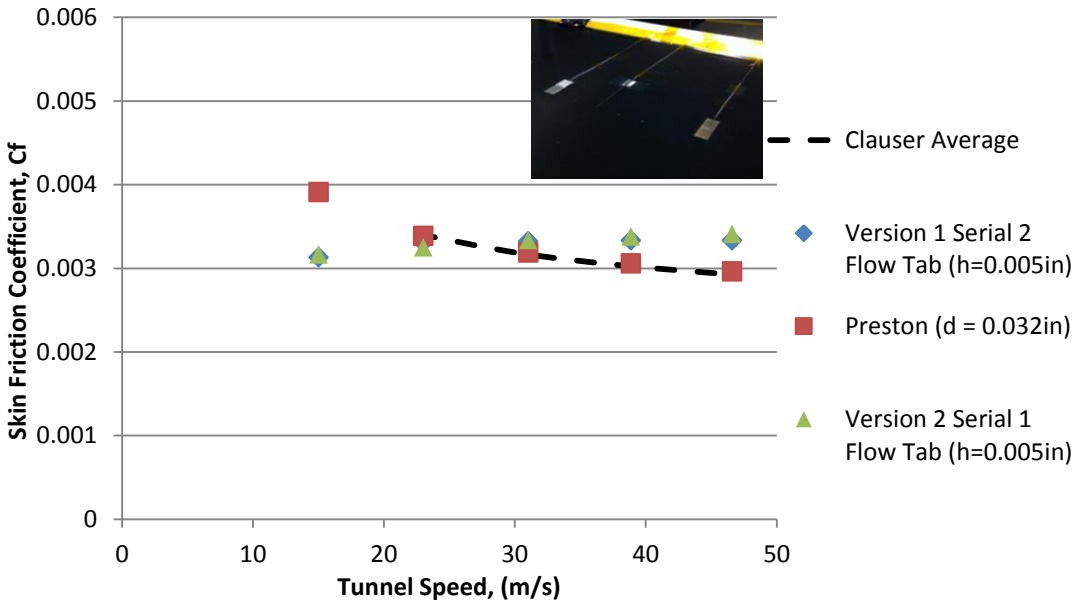

Figure 5-13. Skin friction measurements for Version 1 Serial 2 and Version 2 Serial 1 Flow Tabs in turbulent (tripped) flow (3V1S2-1V2S1-15P-T)

5.5.7 Version 2 Serial 1 Flow Tab Testing (Laminar)

The trip wire was removed from the flat plate, and the Flow Tabs were retested with laminar flow and analyzed using the same calibrations as explained for the earlier laminar flow tests. The resulting skin friction values are plotted in Figure 5-14; good agreement between results for the two different versions of the Flow Tab as well as the Preston tube values is observed.

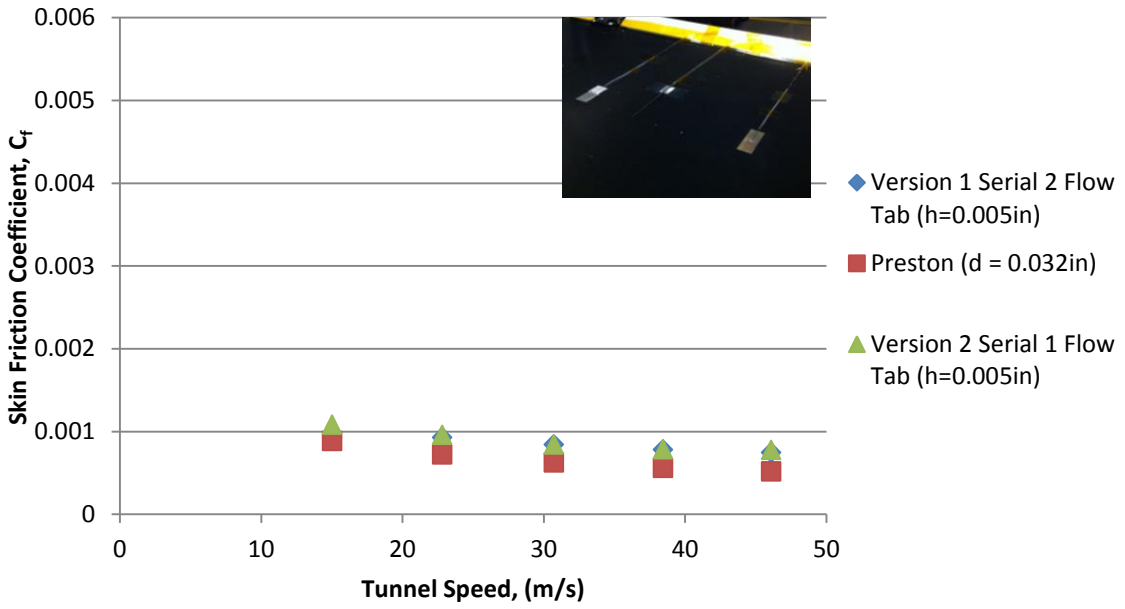

Figure 5-14. Skin friction measurements for V1S2 and V2S1 Flow Tabs for laminar (untripped) flow (4V1S2-2V2S1-16P-L)

5.5.8 Version 3 Serial 1 and Serial 2 Flow Tab Testing

Both of the Version 3 Flow Tabs, serials 1 and 2, were installed on the flat plate at a streamwise location of x = 28 inches. The trip line remained uninstalled for this test in order to collect laminar data from both of the Flow Tabs. The same procedure as well as the same calibration equations were used from the previous experiments conducted. Figure 5-15 shows the relative locations of all of the sensors used in the experimentation. The resulting skin friction coefficients can be seen in Figure 5-16.

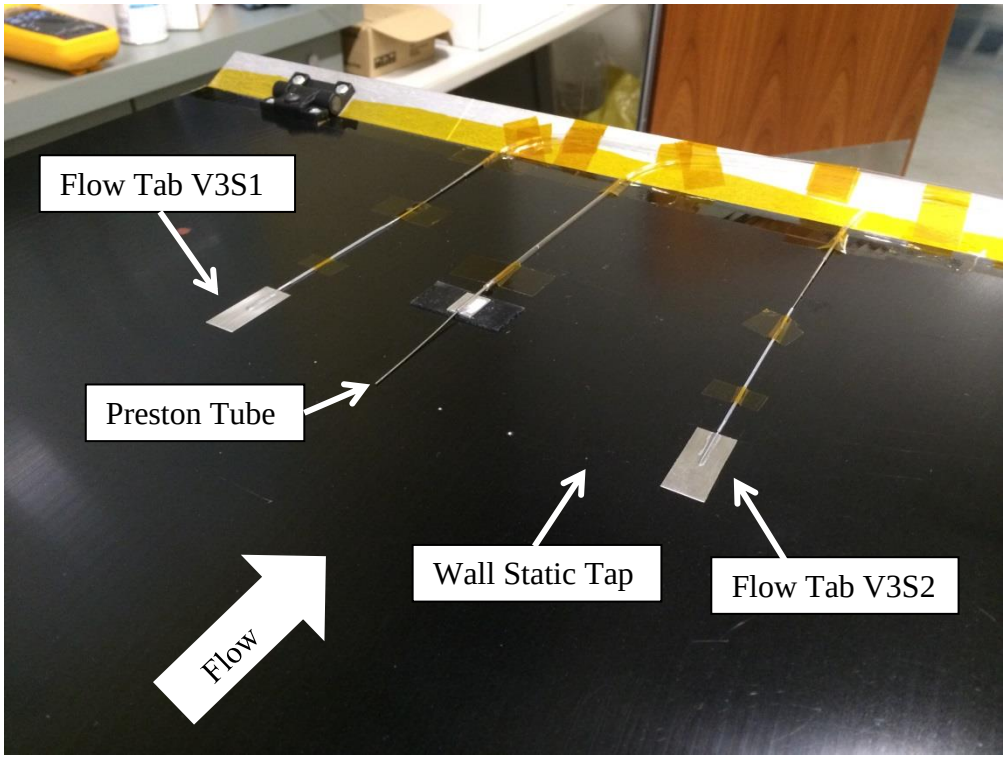

Figure 5-15. Photograph of the test region of the flat plate showing the location of the sensors used for the V3S1 and V3S2 Flow Tab test

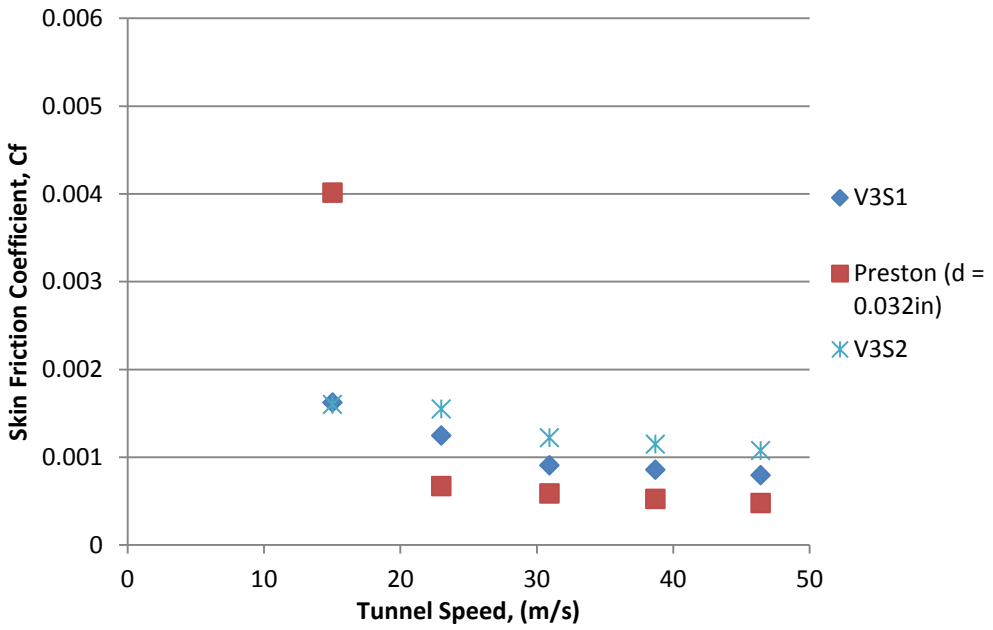

Figure 5-16. Skin friction coefficients at different wind speeds for Flow Tab V3S1 and V3S2 for laminar (untripped) flow (1V3S1-1V3S2-17P-L)

As seen in the results above, both of the Flow Tabs were able to measure data that provide skin friction coefficients that are well within the range of accuracy needed. The results indicate that either blade configuration, either double bevel or single top bevel, would provide skin friction coefficients that would be able to provide the BLDS device with the skin friction coefficients that would be needed to determine flow regime type.

The trip line was subsequently installed on the flat plate at a streamwise location of x = 3 inches to ensure a turbulent flow regime. No other alterations were made to the set up or installation of the previous testing configuration. The resulting skin friction coefficient values can be seen in Figure 5-17.

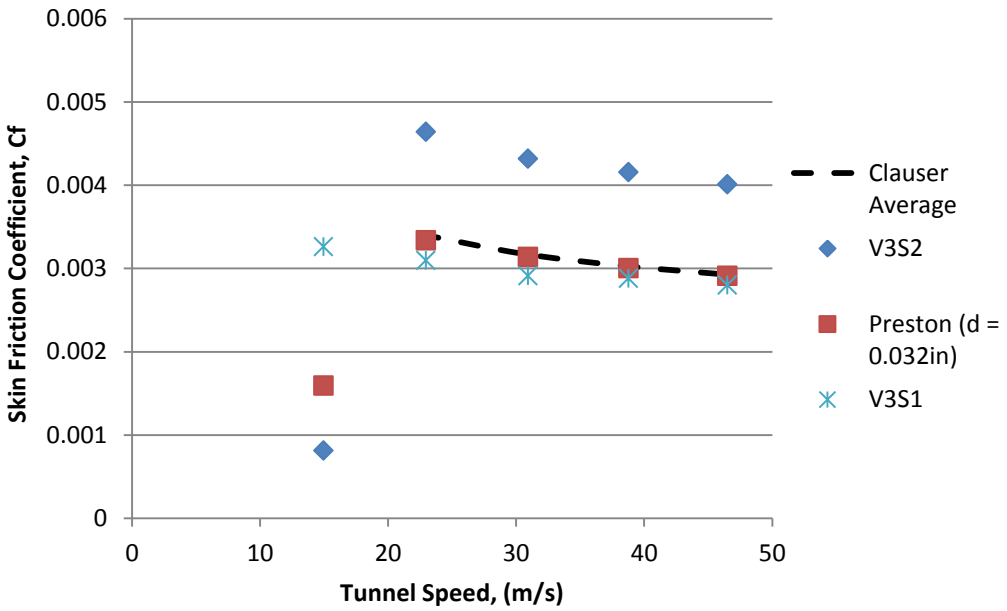

Figure 5-17. Skin friction coefficient at different wind speeds for Flow Tab V3S1 and V3S2 for turbulent (tripped) flow (2V3S1-2V3S2-18P-T)

The results from the turbulent test of the Version 3 Flow Tabs demonstrate that they both provide relatively accurate results for the skin friction coefficient in a turbulent flow regime. The double bevel version, V3S1, provides slightly more accurate results than that of the single top bevel version, V3S2. This is interesting to note and further investigation into this result should be considered. One consideration is being able to verify the as-installed effective height of the Flow Tab once placed on the flat plate. This height is very difficult to precisely measure yet its accuracy is very critical to the calibration equation.

5.6 Summary of the Flow Tab Testing Results

The skin friction measurements presented above for two different versions of the Flow Tab design suggest that the Flow Tab is capable of producing accurate pressure differential measurements that allow for the traditional, accepted Stanton correlations to

be used to provide accurate skin friction measurements. The repeatability of the Flow Tab results was observed to be very good—much better than for earlier testing of a two-piece concept—and the results obtained from the two different versions agreed well with one another. The skin friction measurements from the Flow Tabs agreed well with the Preston tube results, and for turbulent flow, with the Clauser results. In order to provide a datum for comparison for the laminar data results, the solution for laminar flow over a flat plate was used:

$$C_f = \frac{0.664}{\sqrt{Re_x}}$$

Where

$$Re_x = \frac{V\rho x}{\mu}$$

The Reynolds number based on position x, Re_x, of the measurement location was calculated for the laminar data taken with the traditional Stanton gauge and subsequently the skin friction was calculated based on each Re_x value. The laminar results agreed well with the flat plate solution.

The testing for this project was done for a range of Reynolds numbers from about 0.7 to 2.2 million. The various effective heights, h, that were tested throughout the project were made non-dimensional by the inner layer properties. This was accomplished by calculating a non-dimensional height, h+, based on the effective height, h, the shear velocity, u_τ, and the kinematic viscosity, ν:

$$h^+ = \frac{hu_\tau}{\nu}$$

Where:

$$u_\tau = \sqrt{\frac{\tau_w}{\rho}}$$

The range for the non-dimensional heights for all of the testing completed was calculated to be approximately1.4 to 16.

Overall, the Flow Tab design provides an accurate, repeatable way of measuring skin friction on an aerodynamic surface of interest regardless of flow regime. While both Versions 1 and 2 provided comparable results, V2 is much easier to fabricate and install than V1, and will be the recommended Flow Tab configuration for continued future development. V3 follows the same overall design as V2 with the exception of the blade configuration. Both Serial 1 and Serial 2 configurations of the V3 Flow Tab prove to supply fairly accurate results and are both eligible for use on the BLDS. A summary of the results from the various methods of skin friction measurement can be seen in Table 5 and separate plots for skin friction versus wind tunnel speed can be seen for turbulent and laminar flow regimes in Figure 5-18 and Figure 5-19, respectively.

For simplicity of comparing the results, V2S1 Flow Tab is referred to as “Bottom Bevel”, V3S1 Flow Tab is referred to as “Double Bevel”, and V3S2 Flow Tab is referred to as “Top Bevel.”

Table 5-2. Summary of skin friction results from various measurement methods

	Turbulent					Laminar				
	20 Hz	30 Hz	40 Hz	50 Hz	60 Hz	20 Hz	30 Hz	40 Hz	50 Hz	60 Hz
Top Bevel	**Skin Friction Coefficient**					**Skin Friction Coefficient**				
5/13/2014	0.0008	0.0046	0.0043	0.0042	0.0040	0.0016	0.0015	0.0012	0.0011	0.0011
h = 0.002 in	**Speed**					**Speed**				
	14.95	22.95	30.94	38.77	46.49	15.02	23.01	30.95	38.70	46.41
Double Bevel	**Skin Friction Coefficient**					**Skin Friction Coefficient**				
5/13/2014	0.0033	0.0031	0.0029	0.0029	0.0028	0.0016	0.0012	0.0009	0.0009	0.0008
h = 0.0035 in	**Speed**					**Speed**				
	14.95	22.95	30.94	38.77	46.49	15.02	23.01	30.95	38.70	46.41
Bottom Bevel	**Skin Friction Coefficient**					**Skin Friction Coefficient**				
11/9/2013	0.0032	0.0032	0.0033	0.0034	0.0034	0.0011	0.0010	0.0008	0.0008	0.0008
h = 0.005 in	**Speed**					**Speed**				
	15.02	23.01	31.04	38.87	46.60	15.01	22.81	30.71	38.45	46.10
Stanton	**Skin Friction Coefficient**					**Skin Friction Coefficient**				
6/25/13 & 4/29/14	--	0.0039	0.0033	0.0032	0.0033	0.0018	0.0017	0.0012	0.0011	0.0010
h = 0.00175 in	**Speed**					**Speed**				
	--	23.30	31.40	39.47	47.35	14.98	22.79	30.68	38.42	46.06
Preston	**Skin Friction Coefficient**					**Skin Friction Coefficient**				
5/13/2014	0.0016	0.0033	0.0031	0.0030	0.0029	0.0040	0.0007	0.0006	0.0005	0.0005
d = 0.032 in	**Speed**					**Speed**				
	14.95	22.95	30.94	38.77	46.49	14.95	22.95	30.94	38.77	46.49
Clauser Average	**Skin Friction Coefficient**					**Skin Friction Coefficient**				
(turbulent)	--	0.0034	0.0032	0.0030	0.0029	0.0008	0.0006	0.0006	0.0005	0.0005
Flat Plate Solution	**Speed**					**Speed**				
(laminar)	--	22.60	30.40	38.20	45.80	15.02	23.01	30.95	38.70	46.41

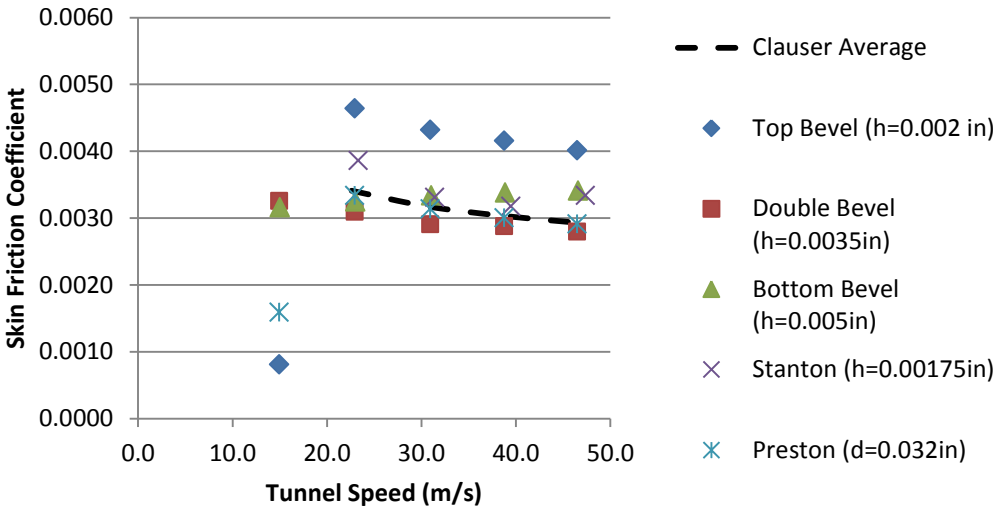

Figure 5-18. Summary of skin friction coefficient versus wind speed for turbulent flow regime

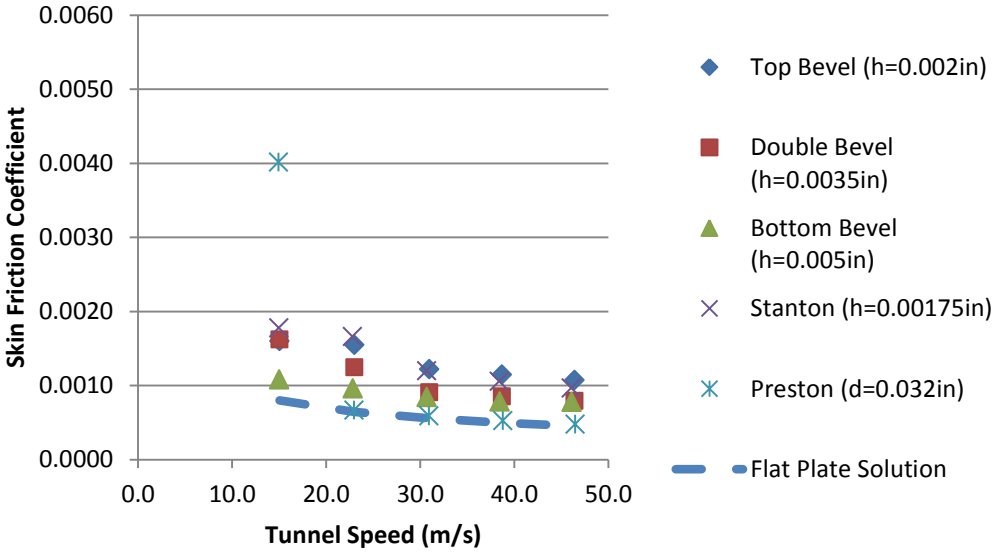

Figure 5-19. Summary of skin friction coefficient versus wind speed for laminar flow regime

6. UNCERTAINTY ANALYSIS

The uncertainty in the various measurements made in order to calculate the resulting skin friction coefficient for each experimental test is evaluated for its effect upon the results of the Flow Tab. There were several aspects of the design that were evaluated in order to determine their respective effects upon the resulting calculation of skin friction coefficient. The variables include: 1) the ambient temperature, 2) the effective height of the razor edge, 3) the static pressure reading, 4) the dynamic pressure reading, and 5) the differential pressure measured between the disturbed and undisturbed statics. All five of these factors were evaluated for their respective uncertainty values as well as their contribution to the overall uncertainty of the measurement of skin friction.

Determining the individual uncertainties in each factor considered was based on manufacturer specifications for the measurement equipment as well as a certain level of experience with taking the respective measurements and what the normal baseline behavior is for the equipment. For the temperature measurement that was taken in the ambient lab conditions surrounding the wind tunnel, it was determined that an uncertainty of approximately 1 degree Celsius would be effective in capturing the distribution of the temperature within the air conditioned environment. The effective height uncertainty was determined to be 0.0005 inch based on the manufacturer's specification on the precision micrometer used to measure the various heights of all of the blades as well as the uncertainty of the as-installed height which could be different from the nominal height of the blade due to various factors. These factors include adhesive transfer tape height after

pressure curing, as well as debris that could be present underneath the tape which could cause the assembly to be offset from the surface an unknown distance.

The pressure measurements made for the ambient static pressure were estimated to have an uncertainty of about 1½ percent. This was decided upon due to the fact that the uncertainty in the measurement stems from the lack of subtracting off the dynamic pressure for each measurement from the stagnation lab reading at the beginning of the test. For the uncertainty in both the dynamic pressure measurements as well as the differential pressure measurements, it was decided that a fixed uncertainty relating to the wind-off readings as well as a variable uncertainty relating to the reading magnitudes themselves was to be used. The wind-off pressure uncertainty was estimated as a fixed 0.0006 V offset for the pressure sensor output voltage readings. This value was converted to the corresponding pressure reading using the calibration constant for the Setra pressure transducer. The variable uncertainty in the pressure measurements taken was estimated at approximately ¼% of each individual reading. This is based on experience with taking the pressure measurements using this particular pressure transducer.

In order to calculate the uncertainty in the skin friction measurements, a sensitivity analysis was completed for each of the variables considered. The skin friction measurement is a function of five variables that are under consideration and is represented by: $C(x_1, x_2, x_3, x_4, x_5)$ where C is the skin friction coefficient and the five x values are the factors under consideration. The total uncertainty in the skin friction measurement is calculated by finding the root sum square of the individual sensitivities of each variable under consideration:

$$u_c = \sqrt{\sum {S_i}^2}$$

Where each individual sensitivity is calculated by using the estimated uncertainty in that particular parameter itself. The skin friction coefficient is calculated twice during this process: once using the nominal value plus the uncertainty, and once using only the nominal value. The difference between these two results is then calculated and it is this difference that is used to calculate the sensitivity of the skin friction coefficient to that particular parameter. This difference is an estimation of the partial derivative of the skin friction coefficient equation with respect to the specified parameter multiplied by the uncertainty in that parameter which is the traditional representation for the uncertainty in the measurement:

$$S_{x_i} = C\left(x_i + u_{x_i}\right) - C(x_i) \approx \frac{\partial C}{\partial x_i} u_{x_i}$$

The sensitivities of each parameter are calculated and tabulated individually and the total uncertainty is calculated from those values. The individual sensitivity values are useful in that they represent the relative effect that each parameter has on the overall uncertainty and therefore highlights areas of measurement that need to be improved in order to improve the overall accuracy in the skin friction measurement. Results from sensitivity analysis on the bottom bevel, double bevel, and top bevel Flow Tab designs can be seen on the following pages. A plot of the nominal data along with error bars representing the calculated uncertainty is shown as well.

Bottom Bevel Flow Tab Uncertainty Spreadsheet

Configuration: Bottom Bevel
Frequency:
Laminar/Turbulent: Turbulent

Uncertainty Uc = sqrt(sxi^2)

Sensitivity Sxi = c(xi+uxi)-c(xi)

Factors Affecting the Uncertainty

	S1	S2	S3	S4	S5	U
20	8.38E-06	-0.00018	-4.7E-06	-1.8E-05	0.000201	0.000268
30	8.1E-06	-0.00017	-4.6E-06	-1.3E-05	6.58E-05	0.000183
40	7.96E-06	-0.00017	-4.5E-06	-1.1E-05	3.26E-05	0.000171
50	7.79E-06	-0.00016	-4.4E-06	-1E-05	2.07E-05	0.000165
60	7.64E-06	-0.00016	-4.3E-06	-9.7E-06	1.53E-05	0.000162

1) Temperature

U 1 deg C

	C(xi+Uxi)	C(xi)	Sxi
20	0.003171	0.003163	8.38E-06
30	0.003256	0.003248	8.1E-06
40	0.003346	0.003338	7.96E-06
50	0.003388	0.00338	7.79E-06
60	0.003417	0.003409	7.64E-06

3) Static Pressure

U 0.005 Percent

	C(xi+Uxi)	C(xi)	Sxi
20	0.003158	0.003163	-4.7E-06
30	0.003244	0.003248	-4.6E-06
40	0.003334	0.003338	-4.5E-06
50	0.003376	0.00338	-4.4E-06
60	0.003405	0.003409	-4.3E-06

5) Delta P

U 0.0006 millivolt
0.0025 Percent

	C(xi+Uxi)	C(xi)	Sxi
20	0.003364	0.003163	0.000201
30	0.003314	0.003248	6.58E-05
40	0.003371	0.003338	3.26E-05
50	0.003401	0.00338	2.07E-05
60	0.003425	0.003409	1.53E-05

2) Effective Height

U 0.0005 in

	C(xi+Uxi)	C(xi)	Sxi
20	0.002987	0.003163	-0.00018
30	0.003079	0.003248	-0.00017
40	0.003171	0.003338	-0.00017
50	0.003217	0.00338	-0.00016
60	0.003249	0.003409	-0.00016

4) Dynamic Pressure

U 0.0006 millivolt
0.0025 Percent

	C(xi+Uxi)	C(xi)	Sxi
20	0.003144	0.003163	-1.8E-05
30	0.003236	0.003248	-1.3E-05
40	0.003327	0.003338	-1.1E-05
50	0.00337	0.00338	-1E-05
60	0.0034	0.003409	-9.7E-06

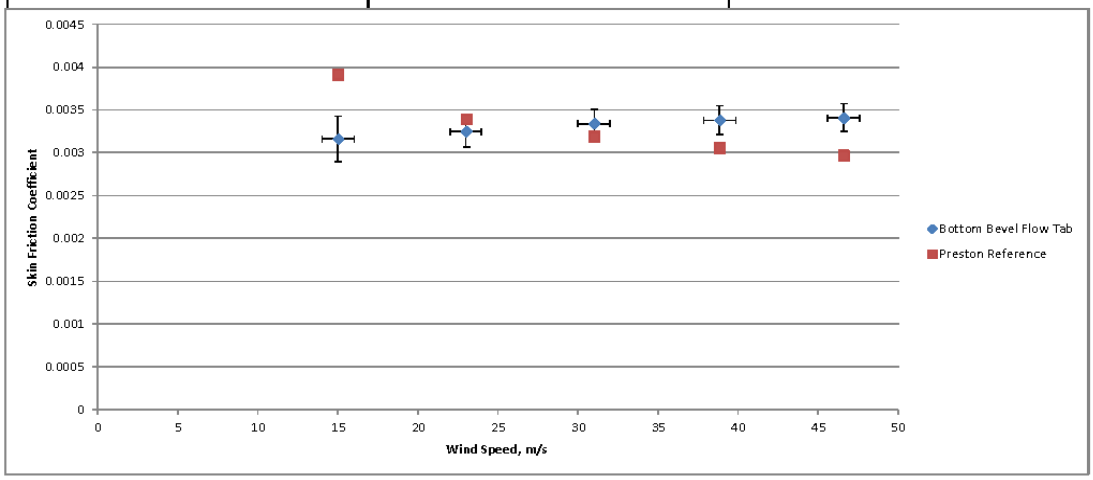

Double Bevel Flow Tab Uncertainty Spreadsheet

Configuration: Double Bevel
Frequency:
Laminar/Turbulent: Turbulent

Uncertainty Uc = sqrt(sxi^2)

Sensitivity Sxi = c(xi+uxi)-c(xi)

	S1	S2	S3	S4	S5	U
20	9.03E-06	-0.00026	-5.1E-06	-1.9E-05	0.000269	0.000376
30	8.12E-06	-0.00024	-4.6E-06	-1.2E-05	8.64E-05	0.000252
40	7.36E-06	-0.00021	-4.2E-06	-9.5E-06	4.15E-05	0.000218
50	7.05E-06	-0.00021	-4E-06	-8.6E-06	2.49E-05	0.000207
60	6.7E-06	-0.00019	-3.8E-06	-8E-06	1.73E-05	0.000196

Factors Affecting the Uncertainty

1) Temperature

U 1 deg C

	C(xi+Uxi)	C(xi)	Sxi
20	0.003268	0.003259	9.03E-06
30	0.003104	0.003096	8.12E-06
40	0.002917	0.002909	7.36E-06
50	0.002886	0.002879	7.05E-06
60	0.002806	0.0028	6.7E-06

2) Effective Height

U 0.0005 in

	C(xi+Uxi)	C(xi)	Sxi
20	0.002998	0.003259	-0.00026
30	0.00286	0.003096	-0.00024
40	0.002696	0.002909	-0.00021
50	0.002674	0.002879	-0.00021
60	0.002605	0.0028	-0.00019

3) Static Pressure

U 0.005 Percent

	C(xi+Uxi)	C(xi)	Sxi
20	0.003254	0.003259	-5.1E-06
30	0.003091	0.003096	-4.6E-06
40	0.002905	0.002909	-4.2E-06
50	0.002875	0.002879	-4E-06
60	0.002796	0.0028	-3.8E-06

4) Dynamic Pressure

U 0.0006 millivolt
0.0025 Percent

	C(xi+Uxi)	C(xi)	Sxi
20	0.00324	0.003259	-1.9E-05
30	0.003083	0.003096	-1.2E-05
40	0.0029	0.002909	-9.5E-06
50	0.00287	0.002879	-8.6E-06
60	0.002792	0.0028	-8E-06

5) Delta P

U 0.0006 millivolt
0.0025 Percent

	C(xi+Uxi)	C(xi)	Sxi
20	0.003528	0.003259	0.000269
30	0.003182	0.003096	8.64E-05
40	0.002951	0.002909	4.15E-05
50	0.002904	0.002879	2.49E-05
60	0.002817	0.0028	1.73E-05

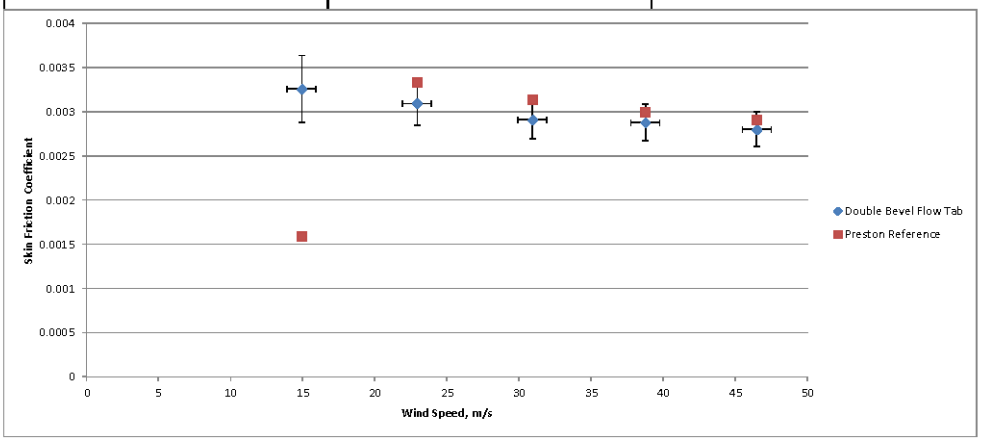

Top Bevel Flow Tab Uncertainty Spreadsheet

Configuration: Top Bevel
Frequency:
Laminar/Turbulent: Turbulent

Uncertainty Uc = sqrt(sxi^2)

Sensitivity Sxi = c(xi+uxi)-c(xi)

	S1	S2	S3	S4	S5	U
20 Hz	7.24E-06	-0.00034	-4.1E-06	-1.4E-05	0.000498	0.000602
30 Hz	1.28E-05	-0.0006	-7.3E-06	-1.8E-05	0.000117	0.000611
40 Hz	1.15E-05	-0.00054	-6.5E-06	-1.4E-05	5.57E-05	0.000543
50 Hz	1.07E-05	-0.00051	-6.1E-06	-1.2E-05	3.34E-05	0.000507
60 Hz	1.01E-05	-0.00048	-5.8E-06	-1.1E-05	2.32E-05	0.000479

Factors Affecting the Uncertainty

1) Temperature

U 1 deg C

	C(xi+Uxi)	C(xi)	Sxi
20 Hz	0.002388	0.002381	7.24E-06
30 Hz	0.004652	0.004639	1.28E-05
40 Hz	0.004331	0.00432	1.15E-05
50 Hz	0.004168	0.004157	1.07E-05
60 Hz	0.004022	0.004012	1.01E-05

3) Static Pressure

U 0.005 Percent

	C(xi+Uxi)	C(xi)	Sxi
20 Hz	0.002376	0.002381	-4.1E-06
30 Hz	0.004632	0.004639	-7.3E-06
40 Hz	0.004313	0.00432	-6.5E-06
50 Hz	0.004151	0.004157	-6.1E-06
60 Hz	0.004006	0.004012	-5.8E-06

5) Delta P

U 0.0006 millivolt
0.0025 Percent

	C(xi+Uxi)	C(xi)	Sxi
20 Hz	0.002879	0.002381	0.000498
30 Hz	0.004756	0.004639	0.000117
40 Hz	0.004375	0.00432	5.57E-05
50 Hz	0.004191	0.004157	3.34E-05
60 Hz	0.004035	0.004012	2.32E-05

2) Effective Height

U 0.0005 in

	C(xi+Uxi)	C(xi)	Sxi
20 Hz	0.002043	0.002381	-0.00034
30 Hz	0.00404	0.004639	-0.0006
40 Hz	0.00378	0.00432	-0.00054
50 Hz	0.003652	0.004157	-0.00051
60 Hz	0.003534	0.004012	-0.00048

4) Dynamic Pressure

U 0.0006 millivolt
0.0025 Percent

	C(xi+Uxi)	C(xi)	Sxi
20 Hz	0.002367	0.002381	-1.4E-05
30 Hz	0.004621	0.004639	-1.8E-05
40 Hz	0.004306	0.00432	-1.4E-05
50 Hz	0.004145	0.004157	-1.2E-05
60 Hz	0.004	0.004012	-1.1E-05

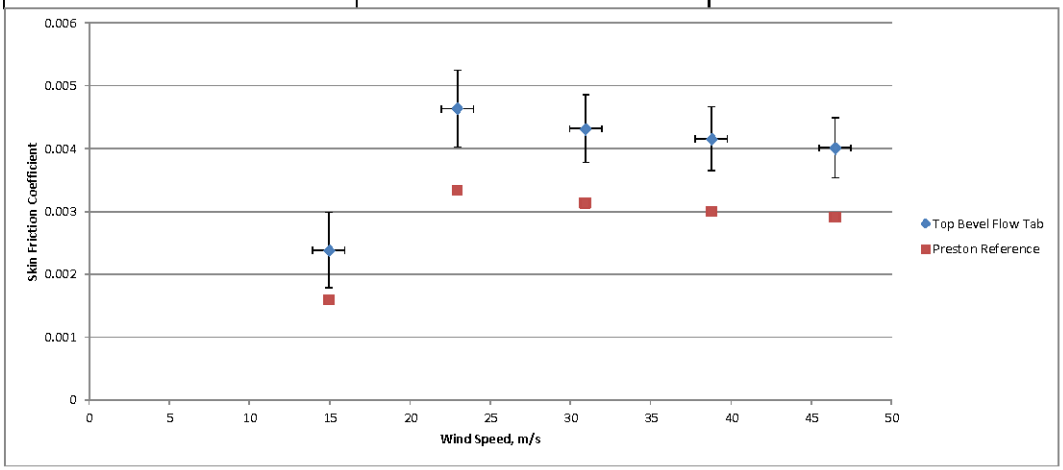

7. CONCLUSIONS & RECOMMENDATIONS

This thesis presented a new method for measuring the skin friction on an aerodynamic surface for the Boundary Layer Data System based on the Stanton method. It allows for a simple and straightforward calculation of the skin friction coefficient and, based upon the magnitude of the coefficient, the flow regime can subsequently be determined. Logistical issues with the implementation of a true Stanton gauge for measuring skin friction were apparent from the beginning of the project. Due to the restrictions of the BLDS requirements for making measurements on aerodynamic surfaces of interest, it was understood that an alteration to the actual hardware used to collect data would need to be made. Specific areas for redevelopment of the device were ease of installation, and level of necessary alteration to the model's surface.

The Flow Tab design for utilizing the Stanton method for measuring skin friction on an aerodynamic model surface is desirable for use on the BLDS device. The design itself has proven to provide measurements that are well within the required/desired accuracy that is needed for both measuring the skin friction values themselves as well as determining the flow regime. The Flow Tab design provides a method for measuring the skin friction on a surface without prior knowledge of the flow regime or the trial and error present with the current use of the Preston method.

Some of the main conclusions that have been reached for this project include various aspects of both the design itself as well as implementation into the BLDS device.

These conclusions are as follows:

1. The Flow Tab design successfully eliminates the need for a wall pressure port as required by the conventional Stanton gauge ("razor blade") skin friction measurement method. Instead, a cavity and a top-mounted pressure connection are used which give the same disturbed pressure measurements—within about 15% for h=0.0035 and h=0.005 inch cases for turbulent flow—as obtained with the conventional Stanton gauge configuration of the same edge height. Therefore, published Stanton gauge calibrations can be used to compute the skin friction from the disturbed pressure measured by the Flow Tab.

2. The primary contributor to the uncertainty in Flow Tab skin friction measurements is accurate determination of the as-installed effective height h. For the present work, this has been estimated at +/-0.0005 inches, and results in uncertainties in skin friction substantially greater than 10% for edge heights as small as 0.002 inches.

3. The Flow Tab design which utilizes adhesive transfer tape (Version 2 and Version 3) is the easiest to both fabricate and to install.

4. Effective heights as small as 0.002 inches can be obtained using the Flow Tab design and beveling the forward edge either on the bottom, symmetrically, or the top, and varying the thickness of the metal body. A body thickness of 0.003 inches has been used in the prototypes of this thesis, and gave edge heights of 0.002, 0.0035, and 0.005 inches, for bottom, symmetric, and top bevel configurations, respectively.

5. The Sproston-Göksel static pressure probe provides sufficiently accurate surface static pressure measurements to provide the necessary reference pressure for the use with

the Flow Tab (or a traditional Stanton gauge) with Cp values within +/- 0.5% for laminar flow conditions and within +/- 1% for turbulent flow conditions.

6. Simultaneous use of the Flow Tab and a Sproston-Göksel probe will provide the BLDS device with the capability to measure skin friction in laminar, turbulent, and transitional flows using a single, explicit calibration equation. East's calibration equation [8] is recommended for this purpose.

Based on the results of this project and the conclusions drawn, the following are the recommendations for future work to improve the quality of the results:

- The as-installed effective height of the Flow Tab is difficult to verify. A method for measuring this critical height should be explored to improve the accuracy of the calculation of skin friction.
- A pressure sensor with better precision would allow for more accurate measurements of the differential pressure needed to calculate the skin friction coefficient and therefore should be investigated for implementation.
- A system for taking in-flight, wind-off, zero pressure measurements should be investigated in order to improve the overall accuracy of the pressure measurements. Currently the BLDS system takes a wind-off reading prior to and after the experimentation and the average value is used as the wind-off measurement. Having a current wind-off pressure value during each test point during testing would greatly improve the accuracy of the measurements.
- The possible effects of oncoming flow angle with respect to the flow tab for swept wing applications should be investigated.

REFERENCES

[1] R. Westphal, M. Bleazard, A. Bender, D. Frame and S. Jordan, "A Compact, Self-Containting System for Boundary Layer Measurement in-Flight," *AIAA-2006-3828, AIAA Meeting Papers on Disc [CD-ROM],* Vols. No. 10-13, 2006.

[2] T. J. Hanratty and J. A. Campbell, "Measurement of Wall Shear Stress," in *Fluid Mechanics Measurements,* 2 ed., Washington, Taylor & Francis, 1996, pp. 575-648.

[3] S. F. Hoerner, "Fluid-Dynamic Drag," Hoerner Fluid Dynamics, Bakersfield, 1965.

[4] R. J. Hakkinen, *Survey of Skin Friction Measurment Techniques,* Dayton: AIAA Minisymposium, 1991.

[5] J. C. White, "High-Frame-Rate Oil Film Interferometry," California Polytechnic State Univesrity, San Luis Obispo, 2011.

[6] T. Stanton, D. Marshall and C. Bryant, "On the Conditions at the Boundary of a Fluid in Turbulent Motion," *Proceedings of the Royal Society of London. Series A, Containing Papers of a Mathematical and Physical Character,* 1920.

[7] J. Hool, "A Simple Method which can be used for Different Fluids and Conditions," *Aircraft Engineering,* vol. 28, no. 2, pp. 52-54, 1956.

[8] L. F. East, "Measurement of Skin Friction at Low Subsonic Speeds by the Razor- Blade Technique," *Aeronautical Research Council Reports and Memoranda,* vol. R&M 3525, 1966.

[9] S. S. Abarbanel, R. J. Hakkinen and L. Trilling, "Use of a Stanton Tube for Skin-Friction Measurements," National Aeronautics and Space Administration, Washington, 1959.

[10] F. M. White, Viscous Fluid Flow, New York: McGraw-Hill, 2006.

[11] H. Li, "Constant Voltage Hot-Wire Anemometry for the Boundary Layer Data System," California Polytechnic State University, San Luis Obispo, 2013.

[12] W. Gracey, "Measurement of Aircraft Speed and Altitude," NASA-RP-1046 , 1980.

[13] J. Sproston and O. Goksel, "The calibration of a surface static tube," *The Aeronautical journal,* vol. 76, pp. 101-103, February 1972.

[14] M. Bleazard, "A research instrument for boundary layer measurement in flight," Washington State University, M.S. Thesis 2006.

APPENDIX A. EXPERIMENTAL SET UP

All experimentation was completed in the California Polytechnic State University Mechanical Engineering wind tunnel, seen in Figure A-1 below. The test section of the wind tunnel has a 2 foot by 2 foot cross section, 4 feet in length.

Figure A-1. Cal Poly Mechanical Engineering Wind Tunnel with sharp-edged flat plate installed in the test section

For the testing applications for this project, an aluminum flat plate was used as a model surface upon which measurements were taken. The flat plate is a 0.25 inch thick plate of aluminum that is 23.9 inches wide and 36 inches in length and is installed in the wind tunnel such that it bisects the test section creating approximately equal areas above and below the plate itself. The leading edge of the flat plate has a bottom-facing bevel at an angle of approximately 14 degrees and an adjustable flap of 1.25 inch chord has been

installed on the flat plate's trailing edge. The flap was installed with the intention of preventing separation on the flow at the leading edge of the flat plate by adjusting the angle that the flap makes with the flat plate surface. There are four mounting legs that allow for the flat plate to be secured to the bottom wall of the wind tunnel. Underneath the two back legs, the ones furthest downstream, a set of four washers are placed between the bottom of the leg and the wind tunnel bottom wall. These spacers, with a total width of 0.240 in, offset the back legs from being flush with the bottom wall surface thus creating a very slight (approximately 0.5 degree) angle of attack that the flat plate makes with the oncoming flow. These spacers are installed in an attempt to prevent slow separation at the leading edge of the flat plate by creating a slight favorable pressure gradient. A picture of the flat plate used can be seen in Figure A-2.

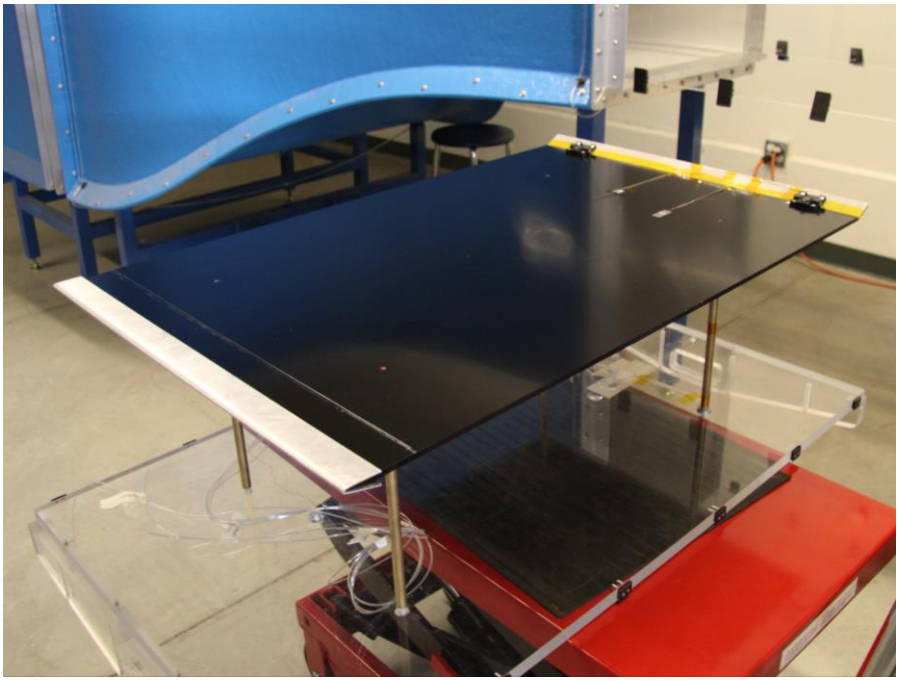

Figure A-2. Aluminum flat plate used as model surface for experimentation

A profile schematic of the flat plate demonstrating the main features of the set up as well as certain locations of importance can be seen in Figure A-3.

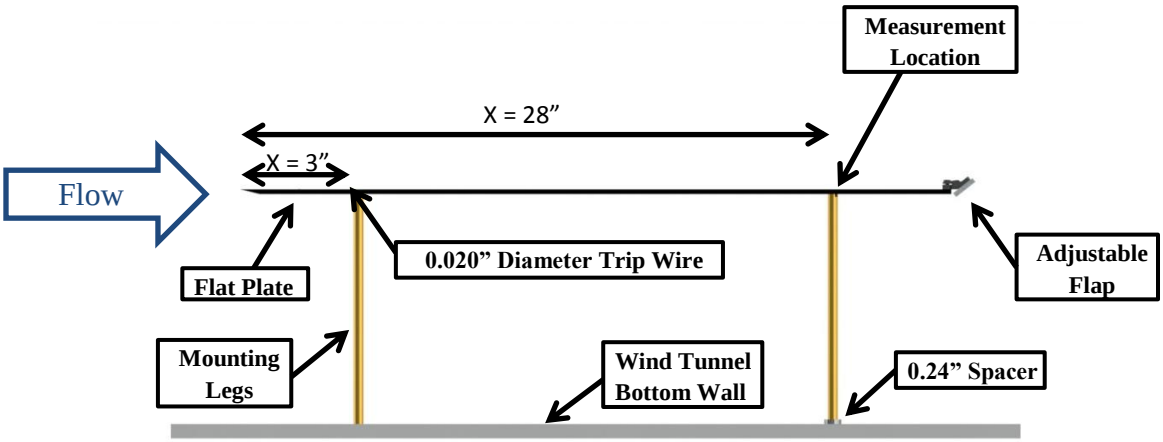

Figure A-3. Flat plate schematic demonstrating important features

For turbulent flow regimes, the trip wire (0.020 in. diameter) was installed on the flat plate in order to trip the incoming flow from laminar to turbulent. For laminar flow regime testing, the trip line was removed in order to have the flow remain laminar along the plate. The static pressure distribution for the flat plate in the wind tunnel is presented in Appendix B.

APPENDIX B. FLAT PLATE STATIC PRESSURE DISTRIBUTION

The static pressure distribution for the flat plate with its current angle of attack with the flow was taken utilizing the same testing configuration as previous testing. The Pitot-static probe was used to measure the dynamic pressure along the centerline of the flat plate approximately 2 inches above the plate's surface. The trip line was not installed for this test in order to achieve laminar flow over the flat plate. A reference location of 3 inches downstream of the flat plate's leading was used to calculate the pressure coefficient at all of the various streamwise locations on the plate itself.

Table B- 1. Dynamic Pressure distribution on flat plate for various wind speeds

	Dynamic Pressure (Pa)				
Streamwise Location (m)	20 Hz	30 Hz	40 Hz	50 Hz	60 Hz
0	122.7	283.1	512.5	798.4	1132.9
0.025	119.7	276.5	502.6	780.9	1105.1
0.051	120.2	277.5	503.8	782.6	1107.4
0.076	120.9	279.3	507.2	788.8	1117.3
0.102	121.7	281.1	510.6	795.0	1127.2
0.152	123.1	284.8	518.1	807.2	1145.8
0.203	124.3	287.6	523.5	816.0	1159.8
0.254	125.2	290.0	528.2	824.2	1172.2
0.305	126.1	292.0	532.1	830.7	1182.5
0.356	127.3	294.2	535.9	836.9	1192.2
0.406	128.1	295.8	539.3	843.1	1202.4
0.457	128.5	297.7	542.1	848.4	1210.3
0.508	129.4	299.1	545.2	853.5	1218.3
0.559	129.9	301.4	547.7	857.7	1225.5
0.610	130.2	302.7	549.4	861.2	1232.0
0.660	130.3	303.0	549.9	862.9	1234.7
0.711	130.1	302.9	549.3	862.7	1234.9
0.762	129.8	302.1	548.2	858.8	1230.1

Table B- 2. Pressure coefficients for the flat plate at various wind speeds

	Pressure Coefficients, C_p				
Streamwise Location (m)	20 Hz	30 Hz	40 Hz	50 Hz	60 Hz
0	0.0145	0.0135	0.0104	0.0121	0.0140
0.025	-0.0104	-0.0099	-0.0092	-0.0100	-0.0109
0.051	-0.0065	-0.0065	-0.0067	-0.0078	-0.0088
0.076	0.0000	0.0000	0.0000	0.0000	0.0000
0.102	0.0065	0.0066	0.0067	0.0079	0.0089
0.152	0.0176	0.0197	0.0214	0.0233	0.0255
0.203	0.0281	0.0298	0.0321	0.0345	0.0381
0.254	0.0355	0.0384	0.0415	0.0449	0.0492
0.305	0.0423	0.0454	0.0491	0.0532	0.0584
0.356	0.0522	0.0534	0.0565	0.0609	0.0671
0.406	0.0590	0.0593	0.0633	0.0689	0.0762
0.457	0.0627	0.0660	0.0689	0.0755	0.0833
0.508	0.0701	0.0708	0.0749	0.0820	0.0904
0.559	0.0745	0.0791	0.0799	0.0874	0.0969
0.610	0.0769	0.0839	0.0832	0.0918	0.1027
0.660	0.0776	0.0850	0.0842	0.0939	0.1051
0.711	0.0757	0.0844	0.0830	0.0937	0.1053
0.762	0.0732	0.0818	0.0808	0.0887	0.1010

A graph demonstrating the pressure coefficients at the various streamwise locations on the flat plate can be seen in Figure B-1 below.

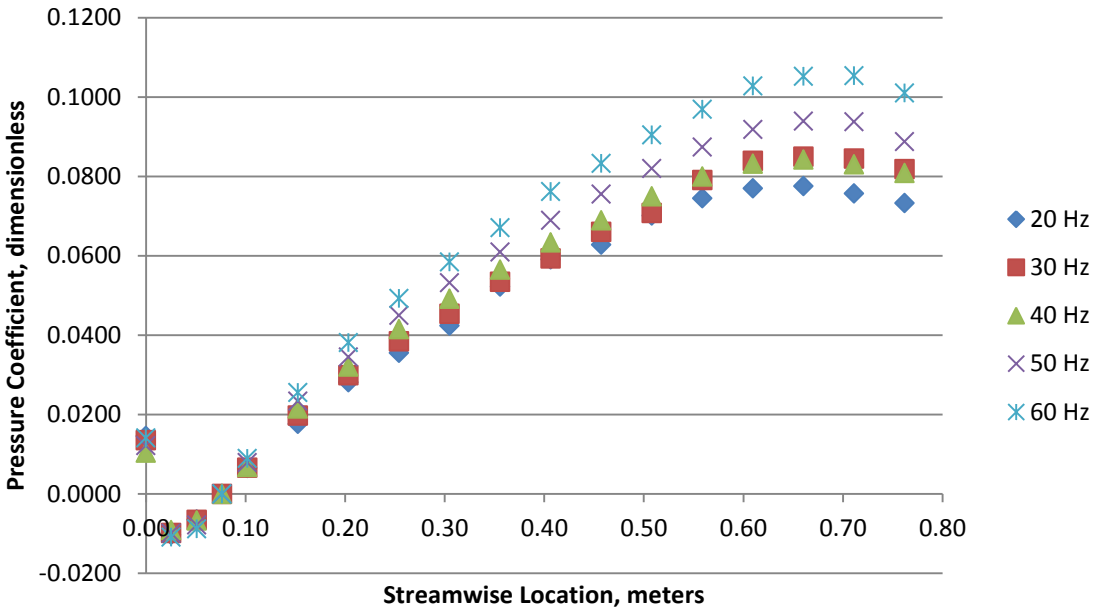

Figure B-1. Pressure coefficients at various streamwise locations on the flat plate at different wind speeds

APPENDIX C. INSTALLATION PROCESS FOR STANTON GAUGES

C. 1 Installation of Two-Piece Prototype Design

The installation process for the initial Stanton Prototype that was developed was the most complicated due to the nature of having two separate pieces that need to be aligned with one another. To begin the process, the U shaped spacer and the main prototype body were cleaned thoroughly with isopropyl alcohol to ensure that the surfaces were clean and that there would be no issues when applying the Duco cement. The two pieces were then aligned with one another and then applied to the surface of the flat plate with the leading edge of the blade aligned at 28 inches downstream of the leading edge. Downward pressure was applied on the prototype as the Duco cement was applied around the side and back edges of the blade assembly. Pressure was maintained for a few minutes as the cement dried to ensure that the cement wouldn't "wick" under the blades and alter the effective height of the assembly. A photograph of the prototype assembly after installation onto the flat plate can be seen in Figure C-1.

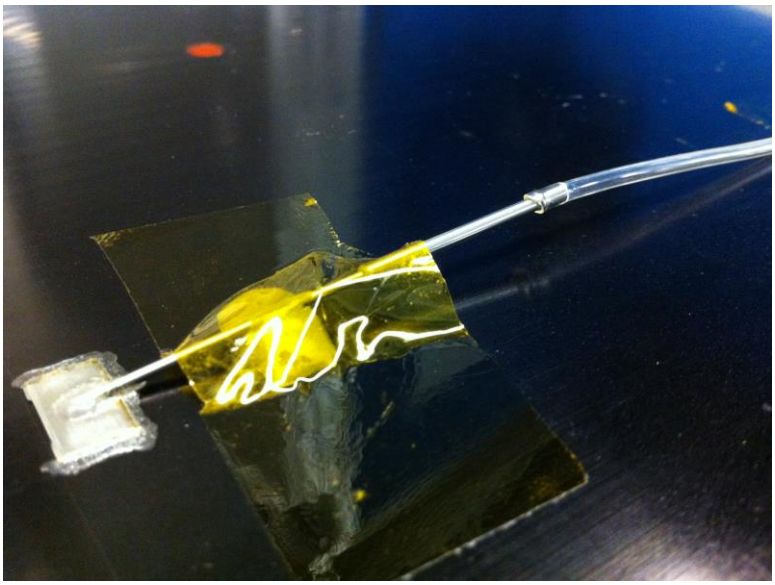

Figure C-1. Prototype assembly after installation on the flat plate

C. 2 Installation of Flow Tab Version 1

The first version of Flow Tab required the use of Duco cement in order to adhere to the model's surface which was achieved in a similar manner to that of the prototype. Due to the delicate nature of the hypodermic tubing on the top of the tab's body, an applicator block was machined out of aluminum in order to ensure that downward pressure was applied to the critical portions of the assembly but not to the delicate sections. A photograph of the block resting atop the Flow Tab can be seen in Figure C-2 below.

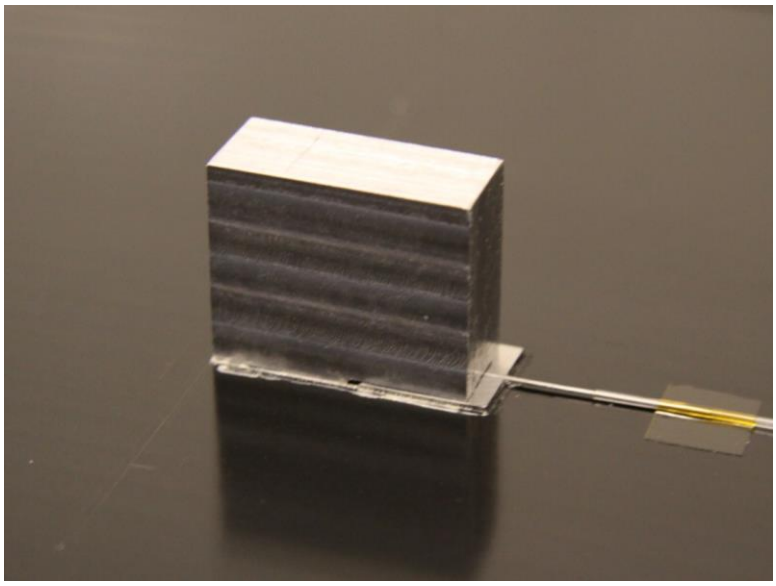

Figure C-2. Applicator block atop Flow Tab Version 1 device

In order to endure that the applicator block was held in place during the adhering process, the block was taped down using masking tape. The tape also applied some downward pressure to the assembly as well which can be seen in Figure C-3 below.

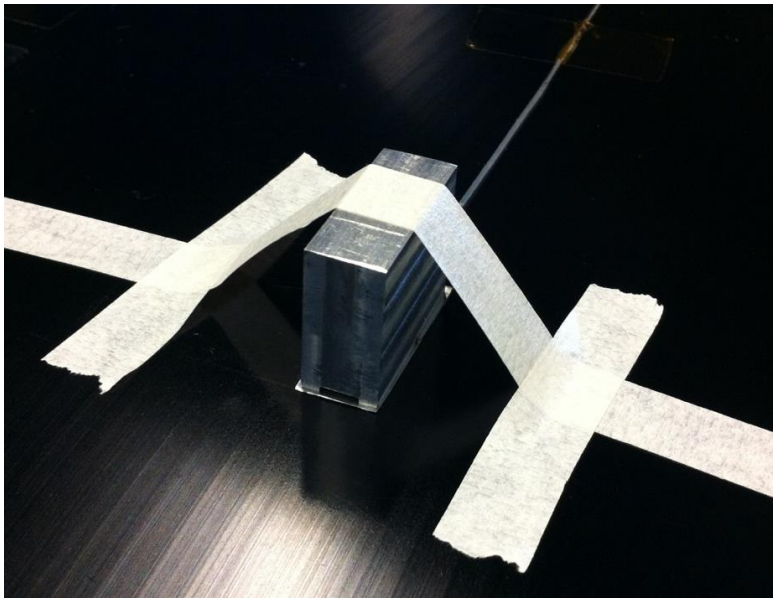

Figure C-3. Applicator block secured in place with masking tape

Downward pressure was applied to the applicator block while the Duco cement was applied to the sides and back of the Flow Tab with a hypodermic needle syringe as shown in Figure C-4 below.

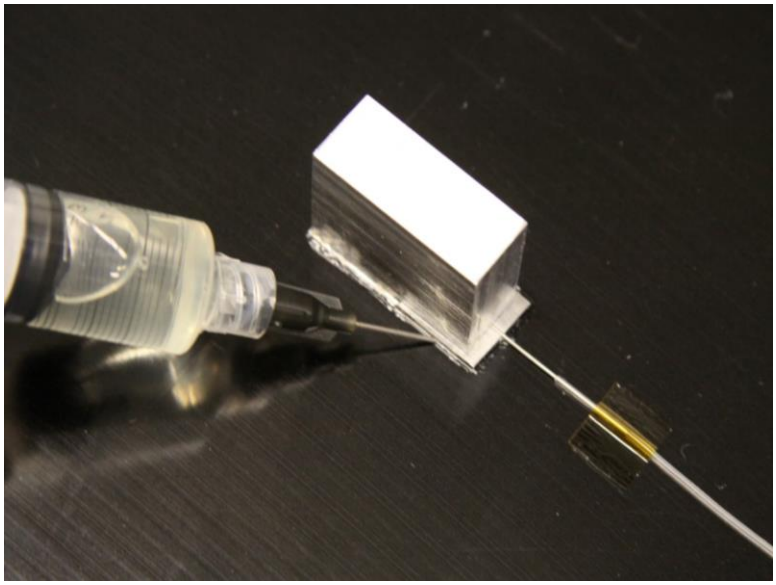

Figure C-4. Application of Duco cement to Flow Tab Version 1 during installation

The assembly was left undisturbed for a period of at least15 minutes to allow the cement to dry. Afterwards, the tape was removed as well as the applicator block and the Flow Tab was ready for testing in the wind tunnel.

C. 3 Installation of Flow Tab Version 2 and 3

With the design change between Version 1 and Version 2 and 3 of the Flow Tab, the installation process changed as well. With the introduction of the adhesive transfer tape to the design, the Duco cement was no longer needed to adhere the tab to the surface. The tape present on the underside of the tab can be seen in Figure C-5 below.

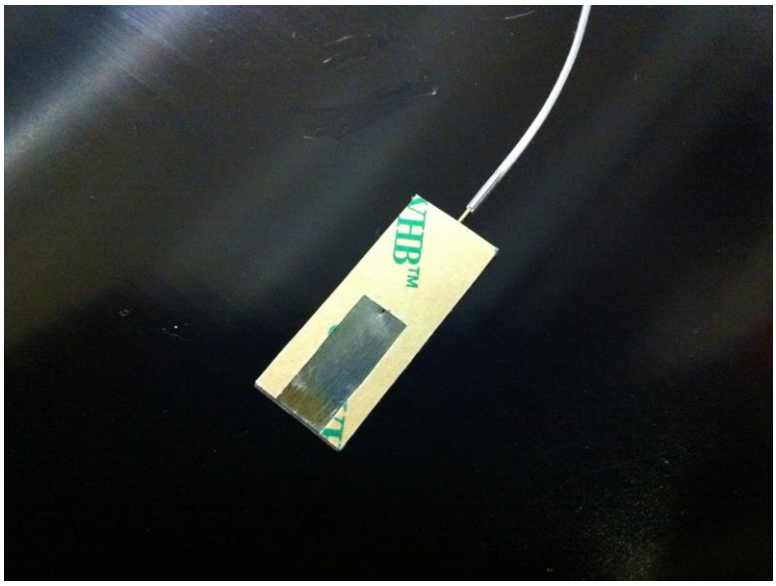

Figure C-5. Adhesive transfer tape on the bottom surface of the Flow Tab

This reduced the complexity as well as the time requirement of the installation process greatly. The tape backing was carefully removed from the bottom of the tab ensuring that the adhesive was not disturbed underneath, seen in Figure C-6.

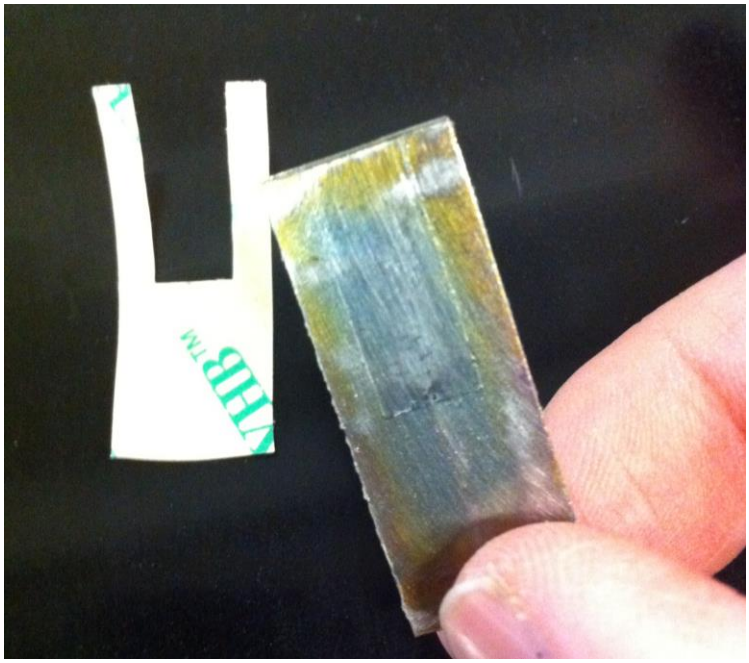

Figure C-6. Adhesive transfer left on the Flow Tab after backing removal

A new applicator block was machined in order to conform to the new design of the top portion of the tab. This block was placed atop the Flow Tab in order to evenly distribute the downward pressure applied by a weight placed atop the block, seen in Figure C-7 and Figure C-8.

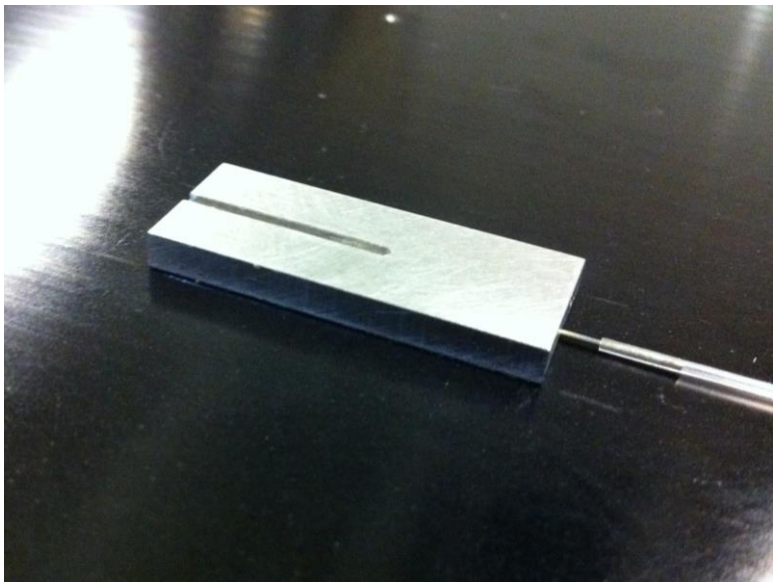

Figure C-7. Applicator block for Version 2 and 3 Flow Tab

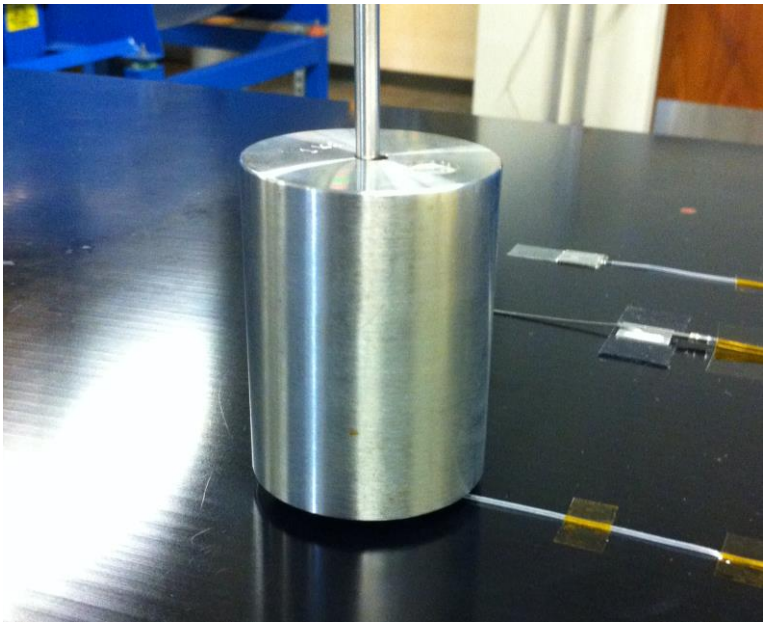

Figure C-8. Weight placed atop the applicator block to apply downward pressure

The weight was left atop the Flow Tab for a period of time in order to allow the adhesive transfer tape to cure. The weight was then removed along with the applicator block and the Flow Tab was ready to be placed in the wind tunnel.

APPENDIX D. TRUE CLAUSER HOTWIRE AND TOTAL PRESSURE DATA

The skin friction data obtained through analysis of velocity profile data using Clauser's method is presented for comparison with the skin friction data measured using Stanton's method. The velocity profile data was measured during the months before the present study, under conditions as nearly as identical to the present study as possible using both hotwire and total pressure probe measurements. The data was obtained by Hon Li in his thesis [11] and a table summarizing his results is seen in Table D-1 below. The uncertainty in the values of skin friction obtained in this manner, using the Clauser method, is believed to be in the range of 5-10% per communication with Dr. Russell Westphal.

Table D-1. Summary of skin friction coefficient values from Clauser analysis

Tunnel Frequency (Hz)	Wind Speed (m/s)	Skin Friction Coefficient, C_f	Method
30	22.6	0.00332	Hotwire
		0.00350	Pressure Probe
40	30.4	0.00309	Hotwire
		0.00327	Pressure Probe
50	38.2	0.00297	Hotwire
		0.00310	Pressure Probe
60	45.8	0.00288	Hotwire
		0.00299	Pressure Probe

The Clauser data will be presented as an average of the hotwire and pressure probe methods for comparison as a true skin friction coefficient value. The skin friction coefficient values from each method are averaged together at each varying wind speed and the resulting values can be seen in Table D- 2.

Table D- 2. Average skin friction coefficient values from Clauser analysis

Tunnel Frequency (Hz)	Wind Speed (m/s)	Average Skin Friction Coefficient, C_f
30	22.6	0.00341
40	30.4	0.00318
50	38.2	0.00304
60	45.8	0.00294

The Clauser data is presented for comparison with experimental results by a dashed curve that runs through the designated points at each wind speed. This line will serve as a datum for other measurements to be compared against for accuracy. There will inevitably be some variation in the test conditions from one experiment to another due to daily fluctuations in laboratory temperature and pressure but this slight discrepancy would lead to such a small contribution to the overall results that the effects will be considered negligible.